Team Persistent or Team Transitory? Sectoral Linkage and Inflation Persistence*

Shu Shen CUHK | Liugang Sheng CUHK | Zhentao Shi CUHK | Steve Pak Yeung Wu UCSD

February 18, 2025

Abstract

The surge in post-COVID-19 inflation has raised critical questions about its persistence and underlying drivers. We employ a high-dimensional Factor-Augmented Vector Autoregression (FAVAR) model, utilizing Lasso techniques to simultaneously capture unobserved common factors, sectoral heterogeneity, and latent intersectoral spillovers. We find that spillovers play a dominant role in sustaining aggregate inflation, surpassing the effects of sectoral heterogeneity and common factors. During the post-COVID period, sector-specific shocks significantly contributed to the variance and persistence of aggregate inflation. Counterfactual analysis reveals that eliminating spillovers would have reduced average post-COVID inflation by 22%, with inflation reverting to the mean three quarters earlier.

Key words: Inflation, inflation persistence, post-COVID inflation, sectoral spillover, Lasso
JEL code: E3, E5

*Shu Shen, shushen@link.cuhk.edu.hk, Department of Economics at The Chinese University of Hong Kong. Liugang Sheng, lsheng@cuhk.edu.hk, Department of Economics at The Chinese University of Hong Kong. Zhentao Shi, zhentao.shi@cuhk.edu.hk, Department of Economics at The Chinese University of Hong Kong. Steve Pak Yeung Wu, stevepywu@gmail.com, Department of Economics at the University of California, San Diego. We thank Michael Devereux, Leland Farmer, Juan Herreno, Zhen Huo, Seung Joo Lee, Zehao Li, Morten Ravn, Walker Ray, Zhesheng Qiu, Alireza Tahbaz-Salehi, Eric Swanson, and the seminar and conference participants for their helpful comments. Sheng thanks the financial support from the Research Grants Council of the Hong Kong SAR (Project No.14501821). All remaining errors are our own.

1 Introduction

The surge in inflation that swept through the United States and the global economy after 2020 has had a significant impact on consumer welfare, raising critical questions for policymakers. Central to these discussions is the issue of inflation's persistence, which has sparked debates and divided opinions into "Team Persistent" and "Team Transitory."

Meanwhile, the COVID-19 pandemic highlighted the crucial role of sectoral disruptions — such as supply chain breakdowns, uneven demand shifts, and intersector spillovers in amplifying economic shocks. This leads to a fundamental question: Are the post-COVID inflationary pressures primarily driven by aggregate shocks or by sector-specific shocks? Moreover, what factors made post-COVID inflation more persistent than initially expected?

The literature on aggregate versus sector-specific sources of inflation has traditionally followed two main approaches. The earlier approach employs dynamic heterogeneous panel models to examine sources of aggregate inflation (Zaffaroni, 2004; Pesaran and Chudik, 2014). These studies highlight the role of sectoral heterogeneity in propagating aggregate shocks (Altissimo et al., 2009; Mayoral, 2013), but often fail to capture sectoral spillovers due to the challenging high-dimensional estimation problem. More recently, structural models incorporating production networks have gained prominence (Guerrieri et al., 2022; Rubbo, 2023; Afrouzi and Bhattarai, 2023), emphasizing how production linkages can amplify inflation persistence. However, these models typically rely on pre-specified production network structures derived from input-output (I-O) tables, which may not accurately reflect the true interconnections that shape sectoral inflation linkages (Li and Martin, 2019).

This paper fills the gap by introducing a high-dimensional, Factor-Augmented Vector Autoregression (FAVAR) model estimated with Lasso shrinkage techniques. This innovative approach enables the empirical decomposition of aggregate inflation into contributions from both aggregate and sector-specific shocks without relying on predetermined production network structures. By leveraging Lasso shrinkage, the model effectively handles the high-dimensionality inherent in sectoral data, allowing for the flexible estimation of latent sectoral spillovers.

Under an aggregate-sector decomposition framework, there are three primary channels manifest through which inflation persistence occurs. First, *common factors* — such as inflation expectations and oil price fluctuations — impact all sectors simultaneously, thus driving widespread inflation persistence (Gagliardone and Gertler, 2023). Second, *sectoral heterogeneity* implies that a skewed distribution of inflation persistence across sectors, where a few sectors exhibit high persistence, can magnify the effects of temporary shocks (Altissimo et al., 2009; Mayoral, 2013). Third, *intersectoral spillovers*, through either production networks or

demand complementarities, can transform temporary shocks into persistent aggregate inflation as they ripple through the economy.

Unlike the two existing approaches, which examine those channels separately, our FAVAR model provides a unified framework to capture these channels flexibly and distinctly. The unobserved common factors capture aggregate shocks affecting all sectors, while the autoregressive coefficient matrix encodes rich information about sector-specific persistence and spillover effects. Specifically, the diagonal elements of this matrix reveal the persistence of inflation within individual sectors, whereas the off-diagonal elements represent the strength and direction of intersectoral spillovers. Mathematically, the persistence of the aggregate inflation impulse response function (IRF) hinges on the largest eigenvalue of the autoregressive coefficient matrix. Intersectoral spillovers can enhance aggregate inflation persistence by increasing the dispersion of these eigenvalues, thereby amplifying the overall inflationary response to temporary shocks.

We apply our FAVAR model to the quarterly PCE sectoral inflation in the United States from 1959 to 2023 for 16 sectors. Our key findings underscore the critical role of intersectoral spillovers for aggregate inflation persistence. First, we observe that the autoregressive coefficient matrix contains 30% non-zero elements, predominantly positive, indicating widespread inflation spillovers across sectors. These effects are particularly pronounced in "hub" sectors like healthcare, recreational goods and vehicles, and food services (food services & accommodations and food & beverages purchased for off-premises consumption), which are central to the spillover network and contribute significantly to aggregate inflation persistence. Furthermore, spillovers increase sectoral granularity, preventing sectoral shocks from averaging out and making them a potentially important source of aggregate inflation dynamics. Second, sectoral inflation persistence driven by spillovers exceeds self-persistence in 11 out of 16 sectors, ultimately dominating inflation dynamics.

Third, counterfactual IRFs, in which we remove spillovers by setting all off-diagonal elements in the autoregressive coefficient matrix to zero, significantly reduce the persistence in the impulse responses of aggregate inflation both for 1% uniform sectoral or aggregate shocks. Specifically, two years after the initial sectoral shocks, the impulse response of aggregate inflation remains at 45 basis points (bps), compared to just 7 bps in the counterfactual IRF without spillovers. Similarly, for the common shock, the impulse response is 12 bps with spillovers but falls to nearly zero bps without them.

Sectoral heterogeneity also plays a role. On top of sector spillover, differences in consumption weights and sectoral self-persistence, captured by the diagonal elements of the autoregressive matrix, increase inflation persistence in two ways. A shock in a sector with high self-persistence has a more prolonged impact, and a shock in a heavily weighted sec-

tor further amplifies aggregate persistence. Empirically, sectors with greater consumption weights, such as "Housing and utilities", tend to exhibit higher self-persistence, reinforcing these effects. Yet, the overall contribution from heterogeneity remains much less significant than spillover effects.

Our framework also accounts for unobserved common factors, which are estimated to be relatively transitory. Statistical tests favor a single common factor, which we find to be highly correlated with oil price changes, with a correlation of 0.47 and 0.78 for the whole sample period and the post-COVID period, and has minimal persistence (an autocorrelation coefficient of 0.02). The sectors most affected by this factor exhibit transitory inflation, underscoring the contrast between common and sectoral shocks.

The above analysis delivers a key message: whether inflation remains transitory or persistent hinges on the relative contribution of these shocks. We conduct a variance decomposition analysis. In the low inflation period such as 2010-2019, common shocks explain about 84% of the total variation. During the early pandemic period in 2020, common shocks also led to a significant decline in inflation. However, from 2021Q2 to 2023, sectoral shocks became more important, accounting for about half of aggregate inflation. The rise in the relative contribution of sector shocks results in more persistent inflation.

Counterfactual analysis highlights the role of spillovers in sustaining post-COVID inflation. Given the estimated shocks and parameters, removing spillovers by shutting down the off-diagonal elements of the autoregressive matrix would have reduced aggregate inflation during the post-COVID period by an average of 22%, with gaps of up to 0.6 log points at the inflation peak. Moreover, aggregate inflation would have reverted to the mean three quarters earlier. By contrast, further shutting down sectoral heterogeneity only slightly changes the aggregate inflation persistence. Finally, an out-of-sample forecasting exercise demonstrates the predictive accuracy of our model, which generates a more realistic and persistent inflation forecast compared to professional forecasters.

Our paper makes an empirical methodological contribution to the literature that examines sector-specific versus aggregate sources of aggregate inflation persistence. To the best of our knowledge, it is the first to provide an econometric framework to estimate the impact of intersectoral spillovers on aggregate inflation persistence. In particular, our approach simultaneously estimates latent sectoral linkages and unobserved common factors, which is crucial for disentangling their respective roles in aggregate inflation dynamics. As noted by Foerster et al. (2011), without accounting for common factors, sector spillovers estimated from a conventional VAR model may be attributed to these unobserved common factors, and the high persistence in sectoral inflation may also be driven by the omitted persistent common factors. Conversely, without accounting for sectoral spillovers, the estimated common factors

in traditional factor models may capture not only aggregate shocks but also idiosyncratic sector-specific shocks propagating through sectoral linkages.

Second, estimating the autoregressive coefficient matrix in the FAVAR model presents challenges due to high dimensionality. For feasible estimation of a high-dimensional FAVAR model that accounts for robust cross-sectional dependence, we employ the Lasso techniques developed by Miao et al. (2023). Lasso (Tibshirani, 1996) has been widely used in econometrics for variable selection, with variants tailored for different tasks (Kock and Callot, 2015; Su et al., 2016; Lee et al., 2022). In our context, more importantly, Lasso serves as a statistical tool to detect latent patterns of intersectoral spillovers. By applying a penalty that shrinks some off-diagonal elements of the autoregressive coefficient matrix toward zero, it shuts off trivial cross-sectoral linkages while highlighting substantial spillovers through the remaining non-zero coefficients.

Lastly, our data-driven approach to estimating sectoral linkages offers distinct advantages over traditional methods, such as imposing sector relationships using a production I-O matrix. Unlike I-O matrices, our model flexibly captures spillovers that extend beyond production-based relationships. For instance, as shown in our analysis, inflation in the healthcare sector generates spillovers to multiple sectors that are not captured in the I-O matrix. Moreover, our approach does not require additional bilateral sectoral data, making it less data-demanding and suitable for real-time applications without data delay and measurement errors.

Literature Review. Our paper contributes to the literature examining sector-specific versus aggregate sources of business cycle variations, following foundational work by Long and Plosser (1987) and Forni and Reichlin (1998). Several studies, such as Barrot and Sauvagnat (2016), Acemoglu et al. (2016), Atalay (2017), Li and Martin (2019), Carvalho et al. (2021) and De Graeve and Schneider (2023), take a more empirical approach to this question. Meanwhile, other research has taken a structural approach to incorporate multisector or production networks into formal models, including works by Gabaix (2011), Acemoglu et al. (2012), Carvalho and Gabaix (2013), Rubbo (2023), Baqaee and Farhi (2020) and Baqaee and Farhi (2019) (see Carvalho and Tahbaz-Salehi (2019) for a recent review.) Our study is closely aligned with Foerster et al. (2011), who demonstrate that an approximate factor model can be derived from a multisector growth model. Our empirical specification is similar; however, due to high-dimensional issues, they directly impose the production I-O matrix as the sector spillover matrix. Our contribution is to address this limitation by employing a statistical tool — the Lasso method, which allows for a more empirically flexible approach to capture latent relationships and extend this understanding to inflation persistence.

The recent surge in U.S. inflation has sparked discussions about its causes. The uneven sectoral pressures and supply chain disruptions during COVID-19 have motivated several discussions on sectoral supply shock implications, including Guerrieri et al. (2022), Borio et al. (2023), Acharya et al. (2023), Comin et al. (2023), Ferrante et al. (2023), and Ascari et al. (2024). Additionally, the Russia-Ukraine conflict has spurred analyses of oil prices and inflation, as discussed by Gagliardone and Gertler (2023) and Kilian and Zhou (2022). Benigno and Eggertsson (2023) and Bernanke and Blanchard (2023) demonstrate that supply-side effects and labor market tightness contribute to the recent inflation surge. Cochrane (2023), Bianchi et al. (2023), Angeletos et al. (2024) and Hazell and Hobler (2024) formulate and deepen the idea of fiscal-driven inflation. Afrouzi and Bhattarai (2023), Afrouzi et al. (2024) and Minton and Wheaton (2023) study the inflation persistence implications in a production network model. We contribute to this discussion by empirically demonstrating the strong relevance of sectoral shocks, the characteristics of specific sectors, and their spillover effects during the post-2020 inflation period.

Layout. We first provide a data description in Section 2. Section 3 describes the econometric model and the estimation procedure. The estimated autoregressive coefficient matrix is presented in Section 4. Sections 5, 6, and 7 provide an analysis of three main channels through which inflation persistence manifests — sectoral spillover, sectoral heterogeneity, and common factors. Section 8 focuses on the post-COVID-19 period and conducts counterfactual experiments and forecast exercises.

2 Data Description

In this empirical application, we apply our econometric methods to the U.S. sectoral inflation. The dataset comprises quarter-on-quarter changes in sixteen sectoral seasonal-adjusted personal consumption expenditure (PCE) price indices. The Bureau of Economic Analysis (BEA) reports those sixteen disaggregated sectoral price indices (at the lowest level) in the NIPA Table 2.3.4, covering four durable goods sectors, four nondurable goods sectors, and eight service sectors. The sample's raw data consists of quarterly observations spanning from 1959Q1 to 2023Q3. Inflation is measured in log percentage points at a quarterly rate,

$$y_{it} = \text{inflation}_{it} = \left(\log \text{PCE}_{it}^{\text{index}} - \log \text{PCE}_{it-1}^{\text{index}}\right) \times 100\%.$$

The sectoral expenditure share weights can be computed using the nominal PCE values in NIPA table 2.3.5. Given the very low-frequency change of the sector weight, for simplicity, we assume that the sector weights are constant across the sample period and equal to the

sample average of the quarterly weights,

$$w_i = \frac{1}{T}\sum_{t=1}^{T} w_{it} \times 100\% = \frac{1}{T}\sum_{t=1}^{T} \frac{\text{PCE}_{it}^{\text{value}}}{\text{PCE}_{t}^{\text{value}}} \times 100\%.$$

Table 1: Summary Statistics of Sectorial Inflation Rates (Unit: %)

Sector	Weight	Mean	Std.	Min	Max
Durable Goods					
Motor vehicles and parts (Motor Veh.)	5.15	0.56	1.09	-1.55	6.74
Furnishings and durable household equipment (Furnishings)	3.44	0.27	0.87	-1.58	3.83
Recreational goods and vehicles (Rec. Goods)	2.89	-0.52	1.04	-3.02	2.21
Other durable goods (Other Dur.)	1.54	0.42	1.09	-1.72	6.97
Nondurable Goods					
Food and beverages purchased for off-premises consumption (Food Bev.)	11.30	0.80	0.99	-1.01	4.64
Clothing and footwear (Clothing)	5.09	0.27	0.86	-5.91	3.06
Gasoline and other energy goods (Gasoline)	3.58	1.06	6.78	-41.77	19.91
Other nondurable goods (Other Nond.)	7.86	0.77	0.71	-0.53	4.71
Services					
Housing and utilities (Housing)	17.86	0.94	0.60	-0.06	2.90
Health care (Health)	12.01	1.18	0.78	-0.33	3.50
Transportation services (Transport)	3.18	0.92	1.00	-2.58	6.03
Recreation services (Recreation)	3.07	0.89	0.47	-0.32	2.87
Food services and accommodations (Food Serv.)	6.45	1.02	0.64	-0.32	3.81
Financial services and insurance (Finance)	6.29	0.99	1.38	-4.09	7.41
Other services (Other Serv.)	8.15	0.92	0.60	-0.18	3.25
Final consumption expenditures of nonprofit institutions serving households (NPISHs)	2.15	0.40	1.51	-4.12	5.26

Notes: This table presents the summary statistics of sectoral inflation of 16 sectors and their expenditure share weights. The sector's abbreviation is shown in parentheses. All sectors have 258 observations of inflation.

The summary statistics of sectoral inflation of 16 sectors and their expenditure share weights are given in Table 1. The three sectors with the largest weight among them are "Housing and utilities" (17.86%), "Health care" (12.01%), and "Food and beverages purchased for off-premises consumption" (11.30%). Over the span of the last sixty years, the average inflation in the services sector has exceeded that of the goods sector. The "Health care" sector, whose weight is the second largest, has the highest average inflation rate of the 16 PCE sectors, reaching 1.18%. Inflation in the durable goods sectors is typically modest, and it has even gone negative for "Recreational goods and vehicles". The sector of "Gasoline and other energy goods" is unique since it experiences exceptionally high volatility (6.78%). Other than that, the inflation volatility of other sectors is roughly about 1%.

3 Econometric Models

We first lay out the general econometric framework in Section 3.1, and then discuss its IRF in Section 3.2. Section 3.3 describes the Lasso procedure that estimates the model, and Section 3.4 presents a simple simulation exercise to show the effectiveness of our estimation.

3.1 High-dimensional VAR Model with Common Factors

For a generic positive integer m, we denote $[m] \equiv \{1, \ldots, m\}$. Let y_{it} be the inflation of the i-th sector at time t, and a total of N sectors are stacked into $\mathbf{Y}_t = (y_{it})_{i\in[N]}$. We write a VAR($p$) model as

$$\mathbf{Y}_t = \sum_{k=1}^{p} \mathbf{A}_k \mathbf{Y}_{t-k} + \boldsymbol{\mu} + \mathbf{e}_t, \quad t \in [T], \tag{1}$$

where $\boldsymbol{\mu} = (\mu_i)_{i\in[N]}$ is the individual-specific heterogeneity (fixed effects), $\mathbf{e}_t = (e_{it})_{i\in[N]}$ is the vector unobservable error term. The slope coefficients are encoded by a $N \times N$ coefficient matrix $\mathbf{A}_k = (a_{ijk})_{i,j\in[N]}$ for each $k \in [p]$, To capture potential common shocks, we allow factor structures to enter the error term

$$\mathbf{e}_t = \boldsymbol{\Lambda}\mathbf{f}_t + \mathbf{u}_t,$$

where $\mathbf{f}_t = (f_{lt})_{l\in[r]}$ consists of r latent factors of mean zero, the $N \times r$ matrix $\boldsymbol{\Lambda} = (\lambda_{il})_{i\in[N],l\in[r]}$ stores the factor loadings, and $\mathbf{u}_t = (u_{it})_{i\in[N]}$ is the vector of idiosyncratic shocks. To identify the VAR coefficients $\mathbf{A}_k$ for $k \in [p]$, we assume $E[\mathbf{u}_t|\mathbf{Y}_{t-1}, \ldots, \mathbf{Y}_{t-p}, \mathbf{f}_t, \boldsymbol{\mu}] = \mathbf{0}$.

Our model features unobserved common factors. The common factors are used to capture unobserved common shocks including oil price shocks, monetary policy, fiscal policy, inflation expectations, TFP shocks, and news shocks, etc. The associated factor loading reflects the contemporary sensitivity of sectoral inflation in response to the common factors. Previous VAR studies for the dynamics of sectoral inflation usually adopted the textbook vanilla VAR and thus may omit important common shocks in the context, leading to potentially biased estimation, pseudo-persistence in sectoral inflation, and spurious correlation between sectoral inflation. For example, the high correlation between sectoral inflation may be caused by a common factor, and high persistence in sectoral inflation may be driven by a persistent common factor Foerster et al. (2011). Moreover, the separation of the common shocks and sectoral shocks allows us to explore the impulse responses of aggregate and sectoral inflation.

3.2 Impulse Responses

We use impulse responses to measure the persistence of sectoral and aggregate inflation, as Mayoral (2013) show that the average of the sectoral IRFs to common shocks is identical to the aggregate IRF to common shocks, while averages of other popular scalar measures of persistence, such as the sum of the autoregressive coefficients (SAC), the largest autoregressive root (LAR), and the half-life (HL), tend to be different from the aggregate level.

It is the most transparent to illustrate the impulse responses from our model by a simple VAR(1) with a single factor. This simple model is also sufficient for our purpose, since our estimation procedures, described in Section 3.3 and detailed in Appendix A, will select $\widehat{r} = 1$ and $\widehat{p} = 1$ given the data in Section 2. Moreover, as the intercept plays no role in IRF, we further suppress the fixed effects $\boldsymbol{\mu}$ and write the model as

$$\mathbf{Y}_t \quad = \quad \mathbf{A}_1 \mathbf{Y}_{t-1} + \mathbf{\Lambda} f_t + \mathbf{u}_t, \tag{2}$$

where we keep using the upper case $\mathbf{\Lambda}$ here as a $N \times 1$ matrix of factor loadings for the sole common factor. This simplified model is closely related to the models in Altissimo et al. (2009) and Mayoral (2013). They mainly focus on the heterogeneity in the diagonal coefficients $a_{ii,1}$, while ignoring inter-sectoral spillover by suppressing the off-diagonal coefficients $a_{ij,1} = 0$ for all $j \neq i$. Our model captures the heterogeneity in sectoral persistence and the spillover between sectors through the VAR specification. The diagonal coefficients $a_{ii,1}$ in $\mathbf{A}_1$ capture the autoregressiveness of each sector i, and the off-diagonal coefficients capture the impact of the lagged inflation in sector j on the inflation of sector i in period t.

When all eigenvalues of $\mathbf{A}_1$ lie in $(-1, 1)$, we can write the VAR(1) as to the moving average representation

$$\mathbf{Y}_t = \left(\mathbf{I} - \mathbf{A}_1(\mathbb{L})\right)^{-1} \left(\mathbf{\Lambda} f_t + \mathbf{u}_t\right) = \sum_{s=0}^{\infty} \mathbf{A}_1^s \left(\mathbf{\Lambda} f_{t-s} + \mathbf{u}_{t-s}\right),$$

where $\mathbb{L}$ is the lag operator. Define the information set $\mathcal{I}_t = ((\mathbf{u}_s, f_s)_{s=-\infty}^t)$. The conditional expectation is

$$\mathbb{E}_t\left[\mathbf{Y}_{t+h}\right] := \mathbb{E}\left[\mathbf{Y}_{t+h} | \mathcal{I}_t\right] = \sum_{s=0}^{h-1} \mathbf{A}_1^s \mathbb{E}\left[\left(\mathbf{\Lambda} f_{t+h-s} + \mathbf{u}_{t+h-s}\right) | \mathcal{I}_t\right] + \sum_{s=0}^{\infty} \mathbf{A}_1^{h+s} \left(\mathbf{\Lambda} f_{t-s} + \mathbf{u}_{t-s}\right). \tag{3}$$

whose stochastic patterns are characterized by the time series (f_t) and $(\mathbf{u}_t)$. The idiosyncratic error $\mathbf{u}_t$ is routinely assumed to be a martingale difference sequence (m.d.s.) with respect to the natural filtration so that $\mathbb{E}\left[\mathbf{u}_{t+s} | \mathcal{I}_t\right] = 0$ for all $s \geq 1$. As a result, the sectoral impulse

response, defined as the h-period ahead responses of $\mathbf{Y}_t$ to unit changes in $\mathbf{u}_t$ is

$$\mathbf{IRF}_{\mathbf{Y}}^{\mathbf{u}}(h) = \partial \mathbb{E}_t \left[\mathbf{Y}_{t+h}\right] / \partial \mathbf{u}_t' = \mathbf{A}_1^h \tag{4}$$

Sectoral IRFs to sectoral shocks, $\mathbf{A}_1^h$, take the form of an $N \times N$ matrix. Each entry in the matrix represents the IRF of the h-period ahead inflation in the row sector i, Y_{it+h}, in response to a unit idiosyncratic shock u_{jt} from the column sector j. The aggregate inflation is the weighted average of sectoral inflation, $\pi_t = \mathbf{w}'\mathbf{Y}_t$, where $\mathbf{w} = (w_i)_{i=1}^N$ are the consumption basket weights of PCE of N sectors. Thus, the h-period-ahead IRF of aggregate inflation to sectoral shocks

$$\mathbf{IRF}_{\pi}^{\mathbf{u}}(h) = \partial \mathbb{E}_t \left[\pi_{t+h}\right] / \partial \mathbf{u}_t' = \partial \mathbb{E}_t \left[\mathbf{w}'\mathbf{Y}_{t+h}\right] / \partial \mathbf{u}_t' = \mathbf{w}'\mathbf{IRF}_{\mathbf{Y}}^{\mathbf{u}}(h) = \mathbf{w}'\mathbf{A}_1^h \tag{5}$$

is the convex combination of the corresponding sectoral IRFs.

On the other hand, different approaches appear in the literature about how to handle the common factor f_t; Mayoral (2013) take it as static, whereas Altissimo et al. (2009) explicitly model its dynamics. In the modeling step, we allow for persistence in f_t, exemplified by an AR(1) process $f_t = \rho f_{t-1} + \epsilon_t$ with the AR coefficient $\rho \in (-1, 1)$ and $(\epsilon_t, \mathbf{u}_t)$ follows a martingale difference sequence. Under this setting, the sectoral impulse response to a common shock ϵ_t is

$$\mathbf{IRF}_{\mathbf{Y}}^{f}(h) = \partial \mathbb{E}_t \left[\mathbf{Y}_{t+h}\right] / \partial \epsilon_t = \sum_{\ell=0}^{h} \rho^{h-\ell} \mathbf{A}_1^{\ell} \mathbf{\Lambda}, \tag{6}$$

where the convention $0^0 = 1$ is adopted to unify the notation when $\rho = 0$. Each entry of this $N \times 1$ vector represents the IRF of sector i's inflation to a unit common shock. The sectoral IRF now depends on the interaction of the factor loading $\mathbf{\Lambda}$, the VAR(1) matrix $\mathbf{A}_1$ and the persistence ρ of the AR process (f_t). Thus, the IRF of aggregate inflation to the common shock ϵ_t is given by

$$\mathbf{IRF}_{\pi}^{f}(h) = \partial \mathbb{E}_t \left[\pi_{t+h}\right] / \partial \epsilon_t = \mathbf{w}' \sum_{\ell=0}^{h} \rho^{h-\ell} \mathbf{A}_1^{\ell} \mathbf{\Lambda}. \tag{7}$$

This formula shows the complex interplay between the persistence of the common factor and the propagation of the common shock through sectoral linkages, both of them contributing to aggregate inflation persistence.

In our empirical context, following the common practice of large factor model, such as Foerster et al. (2011), we do not take a stance on whether the factor is static or dynamic;

instead, we will directly estimate the factor time series from data. We will observe that the estimated factor indeed has very low persistence, with the estimated AR(1) coefficient 0.025. In view of this fact, it is useful to write down the special case when $\rho = 0$, which simplifies the sectoral and aggregate IRFs to common shocks as

$$\mathbf{IRF}_{\mathbf{Y}}^{f}(h) = \mathbf{A}_1^h \mathbf{\Lambda}, \quad \text{and} \quad \mathbf{IRF}_{\pi}^{f}(h) = \mathbf{w}' \mathbf{A}_1^h \mathbf{\Lambda}. \tag{8}$$

In this case, ρ plays no role, and thus the persistence of the aggregate IRF primarily hinges on the largest eigenvalue $\mathbf{A}_1$. Intersectoral spillovers can enhance aggregate inflation persistence by increasing the dispersion of these eigenvalues, thereby amplifying the overall inflationary response to temporary common shocks.

3.3 Estimation Procedure

The data we employed is a panel containing 258 quarterly time series observations of 16 sectors. As a result, each $\mathbf{A}_k$ has 256 ($= 16 \times 16$) unknown coefficients to be estimated from the data. The high-dimensional nature of the matrices creates challenges related to potential overfitting, spurious relationships, and high variance in the estimation. We introduce our regularization approach with the Lasso-typo penalty in this section.

Since the fixed effects play no role in our analysis, we use $\widetilde{y}_{it}$ to denote the *within-group transformed observation*, that is, $\widetilde{y}_{it} = y_{it} - \bar{y}_i$, where $\bar{y}_i$ is the time average of (y_{it}) for each i. Stack $\widetilde{\mathbf{Y}}_t = (\widetilde{y}_{it})_{i\in[N]}$ into an $N \times T$ matrix $\widetilde{\mathbf{Y}} = (\widetilde{\mathbf{Y}}_1, \ldots, \widetilde{\mathbf{Y}}_T)$. Similarly, we construct the $Np \times T$ regressor matrix $\widetilde{\mathbf{X}} = (\widetilde{\mathbf{X}}_1, \ldots, \widetilde{\mathbf{X}}_T)$, where $\widetilde{\mathbf{X}}_t = (\widetilde{\mathbf{Y}}'_{t-1}, \widetilde{\mathbf{Y}}'_{t-2}, \ldots, \widetilde{\mathbf{Y}}'_{t-p})'$ is an Np-dimensional vector. The unknown objects to be estimated are the $r \times T$ matrix $\mathbf{F} = (\mathbf{f}_1, \ldots, \mathbf{f}_T)$, the $N \times r$ factor loading matrix $\mathbf{\Lambda}$, and the stacked slope coefficients (an $N \times Np$ matrix) $\mathbf{B} = (\mathbf{A}_1, \ldots, \mathbf{A}_p)$. The sum of squared residuals can be written in a compact form as

$$\mathrm{SSR}(\mathbf{\Theta}) = \|\widetilde{\mathbf{Y}} - \mathbf{B}\widetilde{\mathbf{X}} - \mathbf{\Lambda}\mathbf{F}'\|_{\mathcal{F}}^2,$$

where $\|\cdot\|_{\mathcal{F}}$ is the Frobenius norm, and the parameter is $\mathbf{\Theta} = \{\mathbf{B}, \mathbf{\Lambda}, \mathbf{F}\}$.

The choice of regularization method depends critically on the economic context, as it must align with the structural characteristics of the data. In this sense, the specifications proposed by Altissimo et al. (2009) and Mayoral (2013) can be interpreted as a special case of a sparse model, where $p = 1$ and all $a_{ij,1} = 0$ for all $i \neq j$, effectively shutting off cross-sector interactions. Here, "sparsity" refers to the configuration that most elements in $\mathbf{A}_k$ are zero, with only the diagonal elements estimated from the data. Recent studies on I-O production matrix spillovers, such as those by Foerster et al. (2011), Baqaee and Farhi (2018), and

Rubbo (2023), have highlighted the sparse nature of the I-O matrix, which reflects that most industries interact with only a limited subset of sectors.

Inspired by the common use of sparsity to simplify the model estimation in the context of inflation, we adopt a Lass-type procedure to produce a data-driven sparse estimator. Tibshirani (1996)'s Lasso is arguably the most popular and successful method for variable selection in high dimension, and its variants have also been intensively studied in econometrics in recent years (Kock and Callot, 2015; Su et al., 2016; Lee et al., 2022). In particular, for the VAR model with a common factor, we follow Miao et al. (2023) to minimize

$$\min_{\mathbf{\Theta}} \left\{ \frac{1}{2NT} \text{SSR}\left(\mathbf{\Theta}\right) + \frac{\gamma_1}{N} \left\|\text{vec}(\mathbf{B})\right\|_1 + \frac{\gamma_2}{\sqrt{NT}} \left\|\mathbf{\Lambda F}\right\|_* \right\} \tag{9}$$

where "vec$(\cdot)$" vectorizes a matrix into a long vector, $\|\cdot\|_*$ is the nuclear norm, $\gamma_1, \gamma_2 > 0$ are two tuning parameters. The above convex programming problem provides a consistent initial estimator of the slope matrix $\mathbf{B}$. The side effect of the shrinkage is that the bias will not be negligible relative to the variance. To refine this estimator, Miao et al. (2023) proposes a further multi-step estimation procedure. Moreover, in practice the number of lags p and the number of factors r must be determined. We adopt Miao et al. (2023)'s methodology to determine these hyperparameters. The full estimation procedure that leads to the final estimator on which our empirical results are based is technical but has no economic content; therefore it is relegated to Appendix A.

Our econometric model and estimation method have three distinct advantages. First, the Lasso-type method can deal with the high-dimensional problem of estimating the autoregressive coefficient matrix. In our context, the total number of time series is moderate (258 quarters). If we do not impose any regularization on the parameters, the ordinary least squares fitting will exhaust too many degrees of freedom, and thus overfit the noises. Moreover, the conventional OLS estimator cannot detect the sparsity of the autoregressive matrix. Lasso's penalty shrinks coefficients toward zero, sacrificing a bit of finite-sample bias to exchange for a substantial reduction in the variance, thereby balancing the bias-variance trade-off for a small mean-squared error.

Second, the Lasso method, used here to estimate the sparse autoregressive matrix, also serves as a statistical tool to discover latent patterns of inter-sectoral spillover. Lasso detects which cross-sectoral linkages are trivial. Conversely, the remaining non-zero off-diagonal coefficients signify substantial sectoral spillovers. This data-driven approach estimates potential sectoral spillover without requiring prior information about the underlying sectoral linkages, such as an I-O table. To be it clear, we are not the first to use the data-driven method to estimate the unobserved connectedness between individuals based on the panel

VAR framework, and The Lasso-type method has been a standard toolbox; for example, Demirer et al. (2018) adopt a large VAR system (with no common factor) to estimate the network connectedness of financial institutions based on the variance decomposition. Our focus, however, is not on the descriptive network, but on the sectoral spillover of shocks from sectoral and common factors and its contribution to aggregate inflation persistence.

Third, a key challenge in traditional factor models (without VAR) is that estimated common factors may capture not only aggregate shocks but also idiosyncratic sector-specific shocks that propagate through production linkages. To address this issue, Foerster et al. (2011) adopt a two-step approach: first, they develop a dynamic multisector growth model accounting for these linkages and compute a filtered sectoral industrial growth rate to eliminate the propagation effects of idiosyncratic shocks. Second, they apply a standard factor model to the filtered growth rates to estimate the relative contributions of aggregate and sector-specific shocks to the variability of aggregate output. By contrast, our model estimates the sectoral spillover linkage and common factors simultaneously, without relying on the prior knowledge of I-O linkages and the complicated filtering procedure based on the dynamic multisector structural model.

Finally, our FAVAR model offers a unified framework to capture the three primary channels contributing to aggregate inflation persistence: common factor persistence, sectoral heterogeneity, and intersectoral spillover. This model enables us to quantify their individual contributions to post-COVID inflation persistence.

3.4 Simulation

To show the effectiveness of the Lasso method in detecting the hidden inter-sectoral spillover, we conduct a simple simulation exercise in Appendix B. We specify the true autoregressive matrix $\mathbf{A}_1^0$ in Figure A1, where $\mathbf{A}_1^0$ is a sparse matrix with diagonals equal to 0.6 and each row has two additional random cells with a value either 0.2 or -0.2. Figure A2 presents the estimated autoregressive matrix without using Lasso, in which the cells with green rectangles indicate the true values are non-zero. It shows that the off-diagonal estimates are poor, as many cells with zero true values are estimated as non-trivial non-zero values (false positive). In other words, without Lasso, it tends to overestimate the presence of spillovers across sectors. By contrast, the Lasso method performs quite well in capturing the sparsity of the true $\mathbf{A}_1^0$ matrix, as shown in Figure A3. It not only detects all non-zero cells but also captures the majority of cells with zeros. For a few cells with true values equal to zero, it yields non-zero estimates, but many of those estimates are actually close to zero. This simulation exercise and comparison show that the Lasso method is useful for detecting the

underlying inter-sector spillovers.

We summarize the superior performance of the Lasso method with a few statistics in terms of model selection accuracy and root mean squared errors (RMSEs). We further conduct this simulation exercise for 500 replications. According to Table A1, the Lasso method achieves significantly lower RMSEs overall (0.0001) and for nonzero entries (0.0009) compared to the standard method without Lasso, which reports RMSEs of 0.0027 and 0.0038, respectively. This indicates that the Lasso method provides more precise estimates. In terms of the estimation accuracy of non-zero entries and zero entries, both methods achieve a perfect true positive rate (TPR) of 100%, indicating that all non-zero entries of the true matrix $\mathbf{A}_1^0$ are accurately estimated as non-zero. However, there is a stark contrast in the false positive rate (FPR), with the standard method without Lasso reporting an FPR of 100%, suggesting a high rate of incorrectly estimating zero entries as non-zero. In contrast, the Lasso method shows a much lower FPR of 8.96%, indicating a much better performance in penalizing false positives and thus providing a more accurate sparse autoregressive matrix. Overall, the exercise demonstrates the superior performance of the Lasso method in terms of both RMSE and FPR, highlighting its effectiveness in regularization and estimation.

4 Estimated Autoregressive Coefficient Matrix

Before we present our empirical analysis, we must first determine the number of VAR lag p and the number of factors r. Our algorithm takes $r = r(p)$ as a byproduct of a given p, and therefore the key is to choose the number of the VAR lags. Regularization via Lasso ensures that unnecessary higher-order lags are shrunken to zero, which provides a negligible contribution to the criterion function Eq.(9). Each hypothesized p is associated with a growth ratio $GR(p)$ of the aggregate squares of the Frobenius norm of a $\widehat{\mathbf{A}}_k$, defined in Appendix A.2 as the relative contribution of including lags p to the model. When we throw our data into the algorithm, the grow ratio $GR(p)$ is maximized at $\widehat{p} = 1$. Then, the thresholding strategy in Eq.(A1) immediately determines $\widehat{r} = 1$ under $p = 1$. From now on, we will work with the VAR(1) model with a single common factor.

We first present the empirical estimate of the VAR matrix in Eq.(2). We then examine the implications of inflation persistence through three broad channels discussed in the introduction: sector spillovers, sector heterogeneity, and common factors in Sections 5, 6 and 7, respectively, and then we account for the post COVID-19 inflation in Section 8.

As we focus on VAR(1), we use a_{ij}, instead of $a_{ij,1}$, to denote the (i, j)-th element in $\mathbf{A_1}$ to simplify the notation. Figure 1 presents the estimated values of the autoregressive coefficient matrix $\widehat{\mathbf{A}}_1$ using a heat map, where an element, $\widehat{a}_{ij}$, represents the estimated influence of

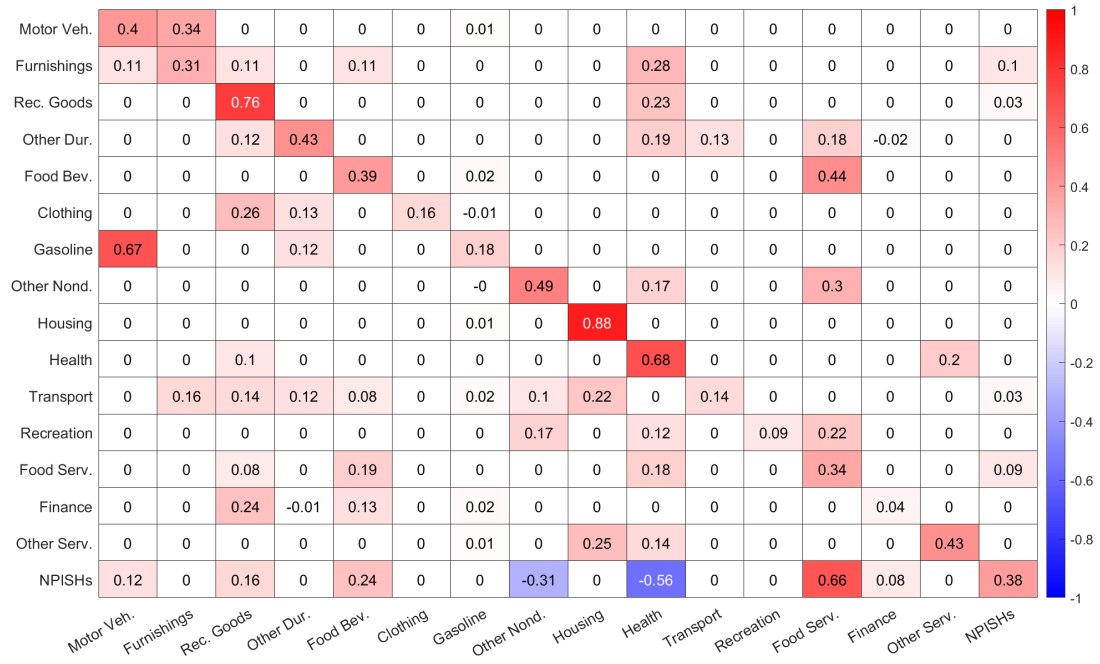


Figure 1: Vector Autoregressive Matrix $\widehat{\mathbf{A}}_1$

Notes: This heat map presents the estimated values of the vector autoregressive coefficient matrix $\widehat{\mathbf{A}}_1$, where an entry $\widehat{a}_{ij}$ represents the estimated influence of the lagged inflation in column sector j on the row sector i's current inflation. Positive and negative values are represented by the red and blue cells and white cells for no impact.

the lagged inflation in column sector j on the row sector i's current inflation. Positive and negative values are represented by the red and blue cells, and white cells indicate no impact.

There are a few noteworthy discoveries. First, 75 out of the 256 total elements are non-zero (about 30 percent), and most non-zero estimates are positive. The Lasso method has reduced some parameters for estimation, thus making the model more parsimonious and offering a conservative estimate of the spillover. Despite that, none of the sectors is isolated. Looking at each row, all sectors' inflation is associated with at least 2 additional sectors. This indicates many important cross-sector relationships.

Secondly, the diagonal elements capture the impact of each sector's inflation in the previous period on its own inflation in the current period. Our estimation suggests that all diagonal elements in $\widehat{\mathbf{A}}_1$ are positive, but the values vary across sectors. This is consistent with the previous literature that finds substantial heterogeneity in sectoral inflation persistence (Altissimo et al., 2009). A high value of the diagonal elements will result in persistent sectoral inflation; however, it should be noted that the diagonal elements do not fully capture sectoral inflation persistence due to the spillover effects across sectors. To ease the

comparison, we rank the sectors by the estimates of $\widehat{a}_{ii}$ from the largest to the smallest in Table A2. It shows that the sectors with high values of $\widehat{a}_{ii}$ are "Housing and utilities" (0.88), "Recreational goods and vehicles" (0.76), and "Health care" (0.68), which tend to have high persistence in sectors' own inflation. By contrast, the "Financial services and insurance," "Clothing and footwear," and "Transportation services" sectors have low values of $\widehat{a}_{ii}$, which tend to have low persistence in their own inflation.

Third, most non-zero off-diagonal elements are positive, indicating a positive inter-sectoral spillover in sectoral inflation. For example, a positive price shock of "Motor vehicles and parts" (0.67 in the first column of Figure 1, perhaps due to demand shock) tends to increase the price of "Gasoline and other energy goods". A positive price shock in "Food services and accommodations" also leads to a hike in the price of "Food and beverages purchased for off-premises" in the next period.[1]

Lastly, Figure A5 in the Appendix E shows the modulus of the eigenvalues of the autoregressive matrix, as some eigenvalues are complex numbers with small imaginary parts. The largest modulus of the eigenvalues is 0.91, higher than the autoregressive coefficient of the housing sector (0.88), indicating the persistence of impulse responses generated from the VAR system.

Comparison with production I-O matrix. We highlight the results in $\widehat{\mathbf{A}}_1$ by comparing them with a more traditional measure, such as the inflation spillover implied by the production I-O matrix. This comparison is non-trivial since the focus here is consumer prices, whereas the production network primarily considers production prices and may omit certain service costs. Nevertheless, we attempt to construct a consumer price spillover matrix derived from the production I-O matrix, denoted as $\widehat{\mathbf{A}}_{IO}$. We make use of the information from the detailed commodity-by-commodity I-O table and PCE bridge table to create $\widehat{\mathbf{A}}_{IO}$. The resulting table is reported in Figure 2 and the detailed procedure for its construction is described in Appendix F.

Several key differences emerge from this comparison. First, as is well-documented in the production network literature, the I-O matrix is highly sparse, reflecting the fact that most products require only a limited range of other products as inputs. This sparsity translates

[1]We find that inflation shocks in "Health care" and "Other nondurable goods" have negative effects on the inflation of final consumption expenditures of nonprofit institutions serving households (NPISHs). This is perhaps due to the measurement of the final consumption expenditures of NPISHs. NPISHs provide various social services, including health care, education, and social welfare to households. Final consumption expenditures by NPISHs is the portion of PCE that represents the services provided to households by NPISHs without explicit charge, which is equal to their gross output (measured as operating costs) less their sales to households. Upon inflation shocks to health care and nondurable goods, the price of the service provided by NPISH to households may increase more than the operating cost of NPISHs as part of their service to households has no explicit charge. In other words, the price of the services that are provided to households by NPISHs without explicit charge decreases.

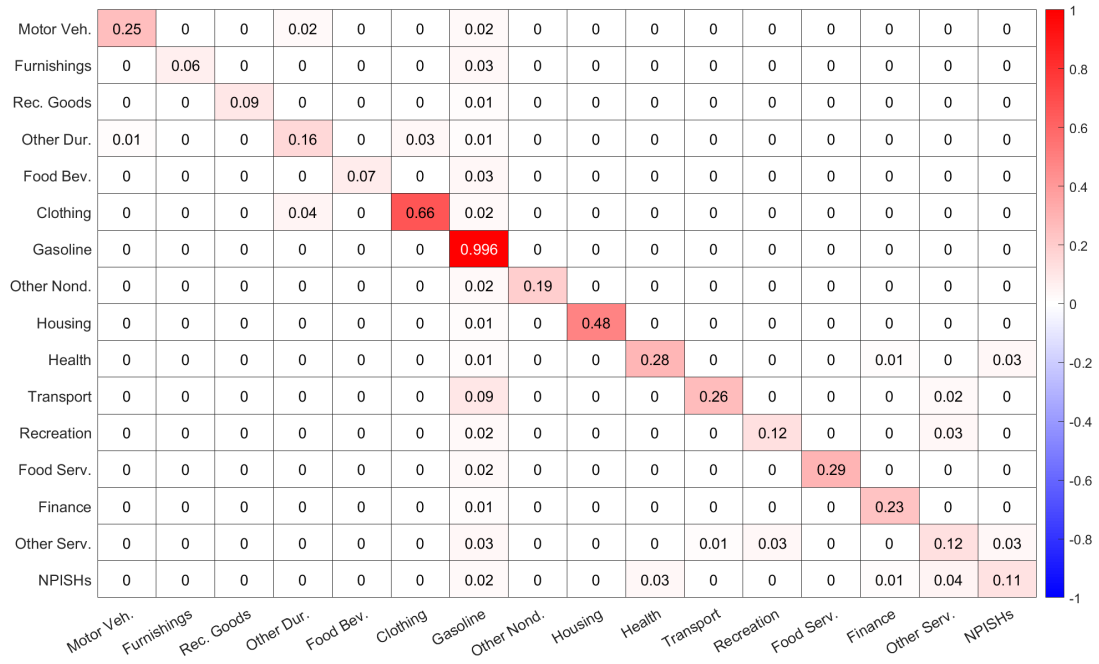


Figure 2: Production I-O Matrix $\widehat{\mathbf{A}}_{IO}$

Notes: This heat map presents the values of the production I-O matrix $\widehat{\mathbf{A}}_{IO}$. Positive and negative effects are represented by the red and blue cells and white cells for no impact.

into a similarly sparse $\widehat{\mathbf{A}}_{IO}$. Specifically, focusing on the off-diagonal elements, only 12% of the entries in $\widehat{\mathbf{A}}_{IO}$ are non-zero, which is relatively low compared to that about 25% in $\widehat{\mathbf{A}}_1$.

Second, we see that some of the spillover that $\widehat{\mathbf{A}}_1$ captures are missed out in $\widehat{\mathbf{A}}_{IO}$. For example, the "Health care" sector and "Food services and accommodations" sectors are almost like an island by itself in $\widehat{\mathbf{A}}_{IO}$. However, $\widehat{\mathbf{A}}_1$ reasonably captures a positive spillover from "Food services and accommodations" to "Food and beverages purchased for off-premises consumption", "Recreation services" and three more sectors. Similarly, "Health care" creates a spillover to eight sectors in total. These findings suggest that $\widehat{\mathbf{A}}_1$ captures broader spillover effects, likely reflecting increases in health care costs, which drive up employee compensation and thereby influence labor costs in production.

Third, the only column that $\widehat{\mathbf{A}}_{IO}$ exhibits a broader sectoral spillover than $\widehat{\mathbf{A}}_{IO}$ is the "Gasoline and other energy goods" sector. As we will explain in detail in Section 7.1, oil and energy price effects are captured as a common factor in Eq.(2). Therefore, the high spillover of the gasoline sector is present in $\widehat{\mathbf{A}}_{IO}$ but not $\widehat{\mathbf{A}}_1$. In sum, the findings here indicate $\widehat{\mathbf{A}}_1$ captures additional latent spillover relationships that go beyond the $\widehat{\mathbf{A}}_{IO}$.

5 Inflation Persistence Implication of Sectoral Spillover

This section demonstrates that sectoral spillovers are a significant driver of inflation persistence. We analyze the implications of sectoral shocks on both sectoral and aggregate inflation persistence through the lens of sectoral spillovers. First, we present a directional network graph to provide an overview of the spillover dynamics. Next, we illustrate sectoral spillovers using four specific examples. Finally, we highlight the importance of sectoral spillovers across nearly all sectors and identify a few "VIP" sectors that play particularly critical roles.

To better illustrate sectoral spillovers, Figure 3 presents the estimates of the autoregressive matrix $\widehat{\mathbf{A}}_1$ as a directional network graph. Green circles represent sector PCE weights, while connection thickness indicates the value of $\widehat{a}_{ij}$, with self-loops for diagonal elements $\widehat{a}_{ii}$. Red and blue indicate positive and negative values, respectively, and arrows show the direction of cross-sector spillover. Sectors with more connections are positioned at the center.

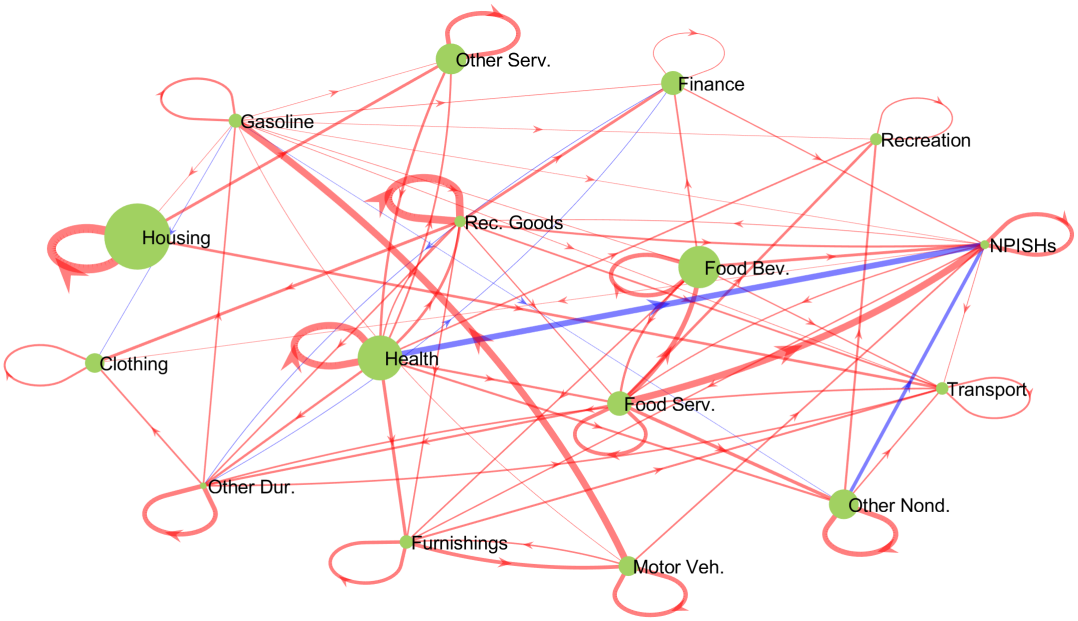


Figure 3: Network Graph of the Autoregressive Matrix $\widehat{\mathbf{A}}_1$

Notes: This directional network graph presents the estimated autoregressive coefficient matrix $\widehat{\mathbf{A}}_1$. Each green circle represents the sector PCE basket weight. The thickness of the connection shows the value of $\widehat{a}_{ij}$ with diagonal elements $\widehat{a}_{ii}$ represented by a self-pointing curve. Positive and negative values are represented by the red and blue curves. The arrow indicates the direction of cross-sector spillover. Sectors that have more connections are presented at the center of the figure.

The network graph reveals two broad types of sectors that contribute more to inflation. The first type is sectors that are highly self-persistent and have a high consumption basket weight. The prime example is the "Housing and utilities" sector. The second type is some "hubs" sectors that are highly centered in the network, significantly influencing inflation

in other parts of the economy via sectoral linkages. These hub sectors include "Health care", "Recreational goods and vehicles", "Food and beverages purchased for off-premises consumption", and "Food services and accommodations".

When these hub sectors experience inflation shocks, the effects rapidly spread to many other parts of the economy through the web of cross-sectoral spillovers. This hub-like behavior suggests that inflation shocks originating in these key sectors can have outsized impacts on aggregate inflation dynamics. The amplification and propagation of inflationary pressures through these intersectoral linkages underscore the importance of accounting for the network-like structure of the economy when analyzing the drivers of sustained high inflation.

5.1 Impulse Responses to Four Selected Sectoral Shocks

To further examine these dynamics, we first study inflation impulse responses of four economically meaningful sectors: "Housing and utilities," characterized by high own persistence and a high consumption basket weight; "Food services and accommodations," notable for high spillovers and a high consumption basket weight; "Health care," distinguished by high own persistence, high spillovers, and a high consumption basket weight; and finally, "Recreational goods and vehicles," which exhibits high own persistence and high spillovers but a low consumption basket weight.

Sectoral Impulse Responses to Four Selected Sectoral Shocks. Figure 4 shows the sectoral inflation impulse responses to a 1% sector shock from four distinct sectors. By definition, a sector shock causes the inflation rate of its own sector to rise by 1% on impact.

As shown in Panel (a) of Figure 4, the "Housing and utilities" shock primarily has a significant and long-lasting effect on its own inflation, remarkably holding half the initial size a year and a half later. This high own-persistence allows the sector to directly transmit inflationary pressures to the aggregate level. Meanwhile, the housing sector's spillover effects, while limited initially, increase gradually over time. Notably, we observe a cascading effect (Acemoglu et al., 2012), as the housing shock first spills over to "Other services" (including household maintenance, personal care, and education service, etc.) and then affects the key "Health care" hub sector, further propagating the inflation pressures. The combination of strong own persistence and growing spillovers underscores the housing sector's outsized influence on aggregate inflation.

In contrast, as depicted in Panel (b), the "Food services and accommodations" sector does not exhibit a strong own-sector response, with its 1% inflation shock dropping to 0.34% after one quarter. However, this sector's shock extends to other sectors, such as "Food services and accommodations" and "Food and beverages purchased for off-premises consumption",

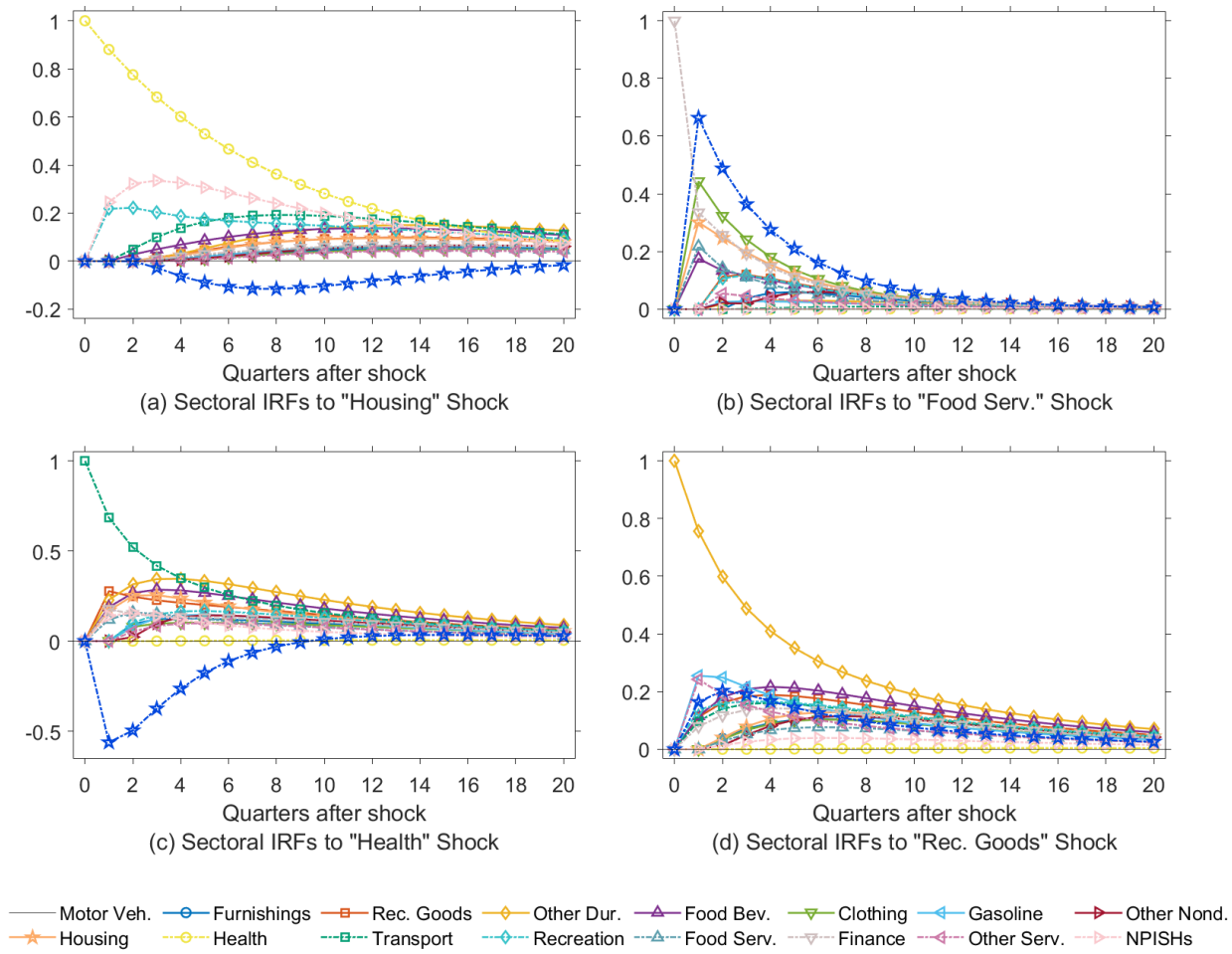


Figure 4: Sectoral Impulse Responses to Four Sectoral Shocks

Notes: This figure presents the impulse responses of 16 sectoral inflation to a 1% sector shock from four distinct sectors (i.e., "Housing and utilities", "Food services and accommodations", "Health care", and "Recreational goods and vehicles") for $h = 0, ..., 20$, derived from the Eq.(4).

with responses even stronger than its own in period 1, indicating powerful spillover effects.

Panels (c) and Panel (d) show that the "Health care" and "Recreational goods and vehicles" sectors play a pivotal "hub" role in the transmission of inflationary shocks. These sectors exhibit a high degree of own-persistence, as seen in their strong self-driven responses, but also widely spread their effects through intersectoral spillovers.

Specifically, the "Health care" shock leads to spillover effects on seven other sectors in the first quarter, offsetting the negative initial reaction of "NPISHs", as shown in Panel (c). The initial shock to healthcare sectors dies out slowly. The rest of the spillover peaks around 4-5 quarters after the shock, leading to persistent inflation.

Similarly, Panel (d) shows that the "Recreational goods and vehicles" shock affects eight other sectors in the first quarter, including "Furnishings and durable household equipment",

"Health care", and "Food services and accommodations". These spillovers then trigger further propagation, as sectors like "Motor vehicles and parts", "Food and beverages purchased for off-premises consumption", and "Recreation services" exhibit subsequent positive responses. These findings underscore the pivotal role played by certain key sectors in amplifying and propagating inflationary shocks through the economy.

Aggregate Impulse Responses to Four Selected Sectoral Shocks.[2] To quantify the implications of the relative importance of the two channels — sectoral self-persistence and spillover effects — on aggregate inflation dynamics, we employ the following decomposition of the aggregate inflation IRFs to a shock in sector i:

$$\underbrace{\mathbf{IRF}_{\pi}^{u_i}(h) \equiv \mathbf{w}'\left(\mathbf{A}_1^h\right)_{\bullet i}}_{\textit{Aggregate IRF to the sector shock}} = \underbrace{w_i\left(\left(\mathbf{A}_1\right)_{ii}\right)^h}_{\textit{own persistence}} + \underbrace{\mathbf{w}'\left(\mathbf{A}_1^h\right)_{\bullet i} - w_i\left(\left(\mathbf{A}_1\right)_{ii}\right)^h}_{\textit{spillover-driven persistence}}, \tag{10}$$

where $\mathbf{w}$ is the vector of PCE consumption basket weight. Figure 5 shows this decomposition for the 1% shocks in the four sectors discussed in Figure 4. The black lines indicate the aggregate inflation IRF to a 1% sector shock. The initial values of the IRF at $h = 0$ do not start at 1% because the origin sector inflation is now multiplied by the sector weight. The blue and red lines represent the breakdown of the aggregate IRF into own persistence and spillover-driven persistence, respectively. The decomposition here clearly quantifies the importance of spillover-driven inflation. The relative importance of the spillover effects increases as the horizon h expands.

For example, in the case of the "Housing and utilities" sector, the own-persistence channel accounts for the majority of the impact on aggregate inflation during the initial quarters. Due to the high own-inflation autocorrelation (0.88), the inflation driven by own persistence lasts for an extended period. However, spillover effects gradually become more influential, rising to nearly half of the total effect by the sixth quarter. The IRF of the "Health care" sector exhibits a similar dynamic, with spillover-driven persistence overtaking its own persistence approximately two quarters after the shock. This is because the own-inflation autocorrelation is lower (0.68), and the spillover effects in health care are more pronounced.

The right panels of Figure 5 show that inflation associated with the "Food services and accommodations" and "Recreational goods and vehicles" sectors exhibit significant persistence even when their own persistence is low. In these IRFs, inflation due to own persistence (blue lines) becomes negligible after 2-3 quarters, but spillover-driven inflation quickly takes over, resulting in a hump-shaped response and prolonged inflation persistence. The half-life of aggregate inflation is approximately 10 quarters following a "Food services and accommo-

[2]The impulse responses of aggregate inflation to sixteen sectors are reported in Appendix G.

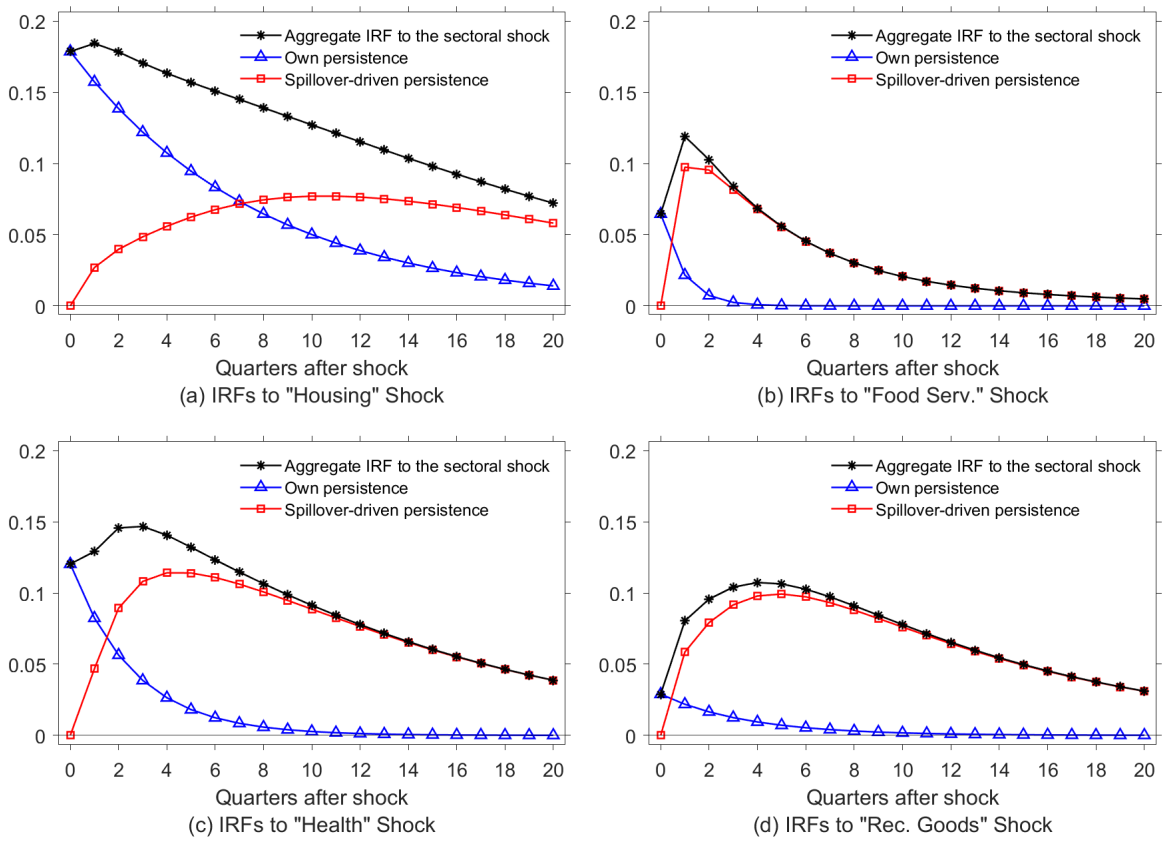


Figure 5: Decomposition of Aggregate IRFs to Four Sectoral Shocks

Notes: This figure presents the decomposition of aggregate inflation impulse responses to a 1% sector shock from four distinct sectors (i.e., "Housing and utilities", "Food services and accommodations", "Health care", and "Recreational goods and vehicles") for $h = 0, ..., 20$, derived from the Eq.(10). The black lines indicate the aggregate inflation IRF to a 1% sector shock. The initial values of the IRF at $h = 0$ do not start at 1% because the origin sector inflation is now multiplied by the sector weight assigned by the BEA. The blue and red lines represent the breakdown of the aggregate IRF into own persistence and spillover-driven persistence, respectively.

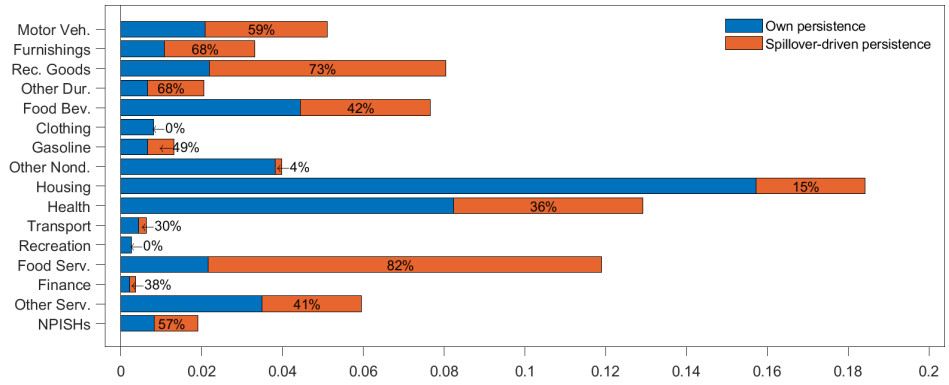
dations" shock and over 20 quarters for a "Recreational goods and vehicles" shock.

5.2 Inflation Persistence Implication of Sectoral Shocks

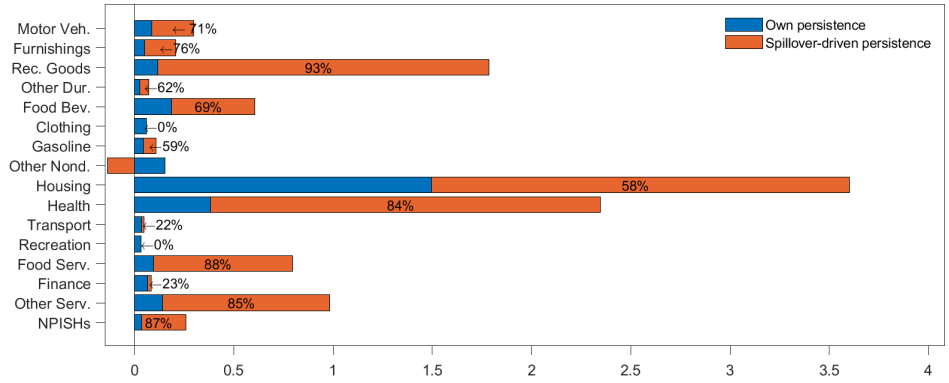
We now summarize the message of Figure 5 for each sector by computing the relative contribution of the sector's own inflation persistence and the spillover-driven persistence to the aggregate inflation IRF. Figure 6 presents aggregate inflation responses to 1% inflation shock to each sector and relative contributions of two channels for the short run (a one-period horizon) and the long run (the sum of infinite periods ahead). For the long-run case, it is equivalent to the area under the curve in Figure 5 as h approaches infinity. The numbers in percentage in the red bars indicate the contribution of the spillover-driven persistence to

the total inflation.

In Panel (a) of Figure 6, we observe that for one period ahead, the spillover-driven persistence accounts for more than 50% of the aggregate inflation response in 6 out of the 16 sectors. The spillover-driven persistence becomes even more dominant in the long run, as shown in Panel (b). For 11 out of the 16 sectors, the spillover-driven persistence exceeds 50% of the aggregate inflation IRF. This highlights the critical role of cross-sector linkages in propagating and amplifying inflationary pressures in the long run.



(a) One-Period Ahead



(b) Sum of Infinite Period Ahead

Figure 6: Decomposition of Aggregate Inflation Responses to Sectoral Shocks

Notes: This figure presents aggregate inflation responses to 1% inflation shock to each sector and relative contributions of two channels (i.e., "Own persistence" and "Spillover-driven persistence", derived from Eq.(10)) for the short run (a one-period horizon) and the long run (the sum of infinite periods ahead). For the long-run case, it is equivalent to the area under the curve in Figure 5 as h approaches infinity. The numbers in the red bars indicate the contribution of the spillover-driven persistence to the total inflation.

Moreover, the x-axis of Figure 6 illustrates the magnitude of the aggregate inflation responses to 1% inflation shock to each sector. For example, aggregate inflation rises by 18 and 13 bps, respectively, one period after the shock to housing and health care. The cumulative long-run inflation effect of these two sectors is more substantial, reaching 3.6% for housing and 2.3% for health care, largely attributable to the spillover-driven persistence.

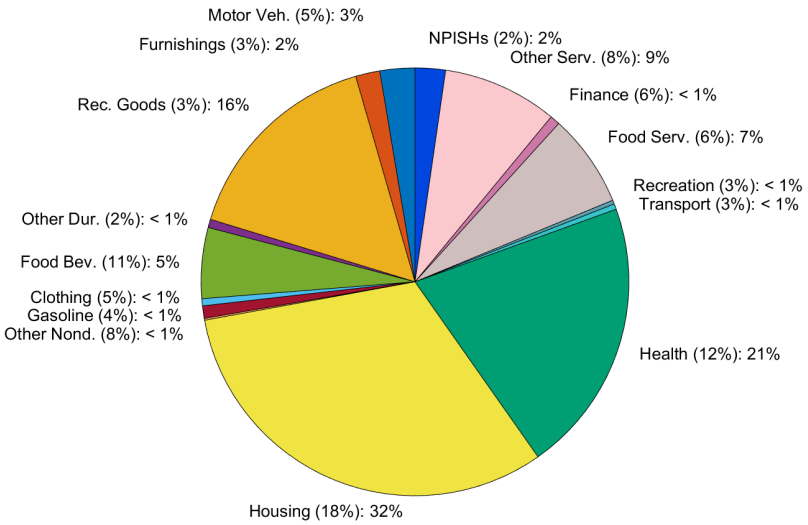


Figure 7: Sectoral Contribution to the Sum of the Infinite Period Ahead Aggregate Inflation IRFs to 1% Inflation Shocks in All Sectors

Notes: This pie chart presents the sectoral contribution to the cumulative sum of aggregate inflation IRFs in infinite horizons to a uniform of 1% inflation shocks in all sectors. Percentages in parentheses indicate the basket weights of each sector. Percentages after the colon indicate the contribution of each sector.

Panel (b) of Figure 6 clearly shows that some sectors, such as housing, are systematically more important in contributing to inflation persistence and long-run inflation. To illustrate this point, we compute the sectoral contribution to the cumulative sum of aggregate inflation IRFs in infinite horizons to a uniform of 1% inflation shocks in all sectors:

$$S_i = \frac{\sum_{h=0}^{\infty} \mathbf{IRF}_{\pi}^{u_i}(h)}{\sum_{i=1}^{N} \sum_{h=0}^{\infty} \mathbf{IRF}_{\pi}^{u_i}(h)}. \tag{11}$$

In other words, we integrate the area under the curve of one IRF and divide it by the sum of the area under the curve for all sixteen sectors' IRF. This is presented in Figure 7. It shows that there are five important sectors, including housing, health care, recreational goods and vehicles, and food (including the sector of food services & accommodations and the sector of food & beverage purchased for off-premises consumption). They contribute about 81% in total for aggregate inflation cumulative responses. Notably, the contribution of those five sectors is much higher than their total weights in the PCE price index listed in Table 1, indicating the heterogeneity in the sector's own persistence and inter-sectoral spillovers may amplify the sectoral granularity, and shocks in those granular sectors could be particularly important for aggregate inflation. However, we should not interpret this result as inflation shocks in other sectors are trivial for aggregate inflation because this exercise assumes the same 1% inflation shock for each sector, while in reality, the sectoral inflation shocks are

certainly heterogeneous.

Our discussion on the granular nature of sectoral shocks is closely related to the notion of "broad-based" supply shocks in Beaudry et al. (2024), where bounded rationality leads households to adjust their inflation expectations in response to broad-base supply shocks that affect many sectors, and thus temporary shocks can have a persistent effect on aggregate inflation in a quasi-self-fulfilling way. Our study complements their theoretical predictions by providing empirical evidence that granular sector shocks, which affect many other sectors through spillover effects, have persistent effects on aggregate inflation.

6 Inflation Persistence Implication of Sectoral Heterogeneity

We now shift our focus to sectoral heterogeneity and its implications for aggregate inflation. Specifically, we examine how differences in sectoral basket weights and sector-specific inflation persistence contribute to overall inflation dynamics. While these aspects of sectoral heterogeneity present interesting economic insights, their implications for inflation persistence are largely overshadowed by the impact of sectoral spillovers.

Even in the absence of inter-sectoral spillovers, inflation can remain persistent if individual sectors exhibit high inflation persistence and if sectors with larger consumption basket weights are disproportionately affected by inflation shocks. As shown in Figure 1, there is substantial variation in sector-specific inflation persistence, with diagonal elements a_{ii} of the $\widehat{\mathbf{A}}_1$ matrix ranging from 0.88 to 0.04. Importantly, when an inflation shock hits a highly persistent sector with a high basket weight, the effect on aggregate inflation persistence is amplified.

Figure 8 illustrates this relationship by plotting sectoral self-persistence coefficients (a_{ii}) against the consumption basket weights assigned by the BEA. The figure reveals a clear positive correlation, with a slope of about 3, indicating that sectors with higher persistence tend to have greater consumption basket weights.[3]

This positive relationship naturally leads to the concept of "systematically more important" sectors in driving inflation dynamics. For instance, a one percent inflation shock in the "Housing and utilities" sector is expected to have a more persistent impact on aggregate inflation due to this sector's combination of the highest consumption weight (18%) and the highest self-persistence (0.88). In contrast, a one percent inflation shock to the "Financial services and insurance" sector is less concerning for aggregate inflation dynamics.

[3]When we estimate the FAVAR model in Eq.(1), consumption basket weight is not provided to the model so there is no mechanical relationship between the self-persistence and consumption basket weight.

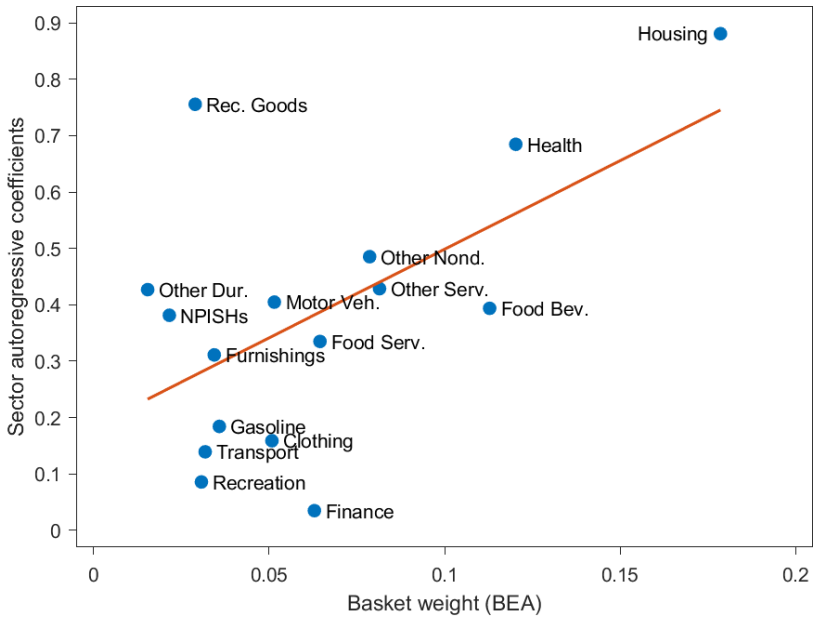


Figure 8: Relationship between Self-Persistence and Consumption Basket Weight

Notes: This scatter plot presents the relationship between sectoral self-persistence coefficients (a_{ii}) and the consumption basket weights assigned by BEA.

This sector not only has a low self-persistence (0.04) but also constitutes a smaller portion (approximately 6%) of the overall consumption basket.

We now demonstrate the relative contributions of sectoral heterogeneity and spillovers to aggregate inflation persistence, showing that sectoral spillovers are the dominant driver. To do so, we compute three hypothetical impulse responses of aggregate inflation to uniform 1% inflation shocks across all sectors and build up the heterogeneity step-by-step. In the first scenario, we shut down all the heterogeneity. We remove both sectoral spillovers and heterogeneity by setting the off-diagonal entries of the estimated matrix $\widehat{\mathbf{A}}_1$ to zero, using the average of the diagonal elements of the estimated autoregressive matrix, $\widehat{\mathbf{A}}_1$, and apply equal basket weights across all sectors to construct a counterfactual autoregressive coefficient scalar, denoted as $\widehat{a}_1^c$. This scenario is referred to as "homogeneous autoregressive without spillover." In the second scenario, we introduce heterogeneous sectoral self-persistence but remove spillovers and apply equal basket weights across all sectors, referred to as "equal weighted heterogeneous autoregressive without spillover." The third scenario isolates the effect of sectoral spillovers by setting the off-diagonal entries of $\widehat{\mathbf{A}}_1$ to zero while keeping both self-persistence and consumption basket heterogeneity, denoted as $\widehat{\mathbf{A}}_1^c$ and labeled "heterogeneous autoregressive without spillover."

We incorporate these three counterfactual matrices into Eq.(5) to derive the corresponding impulse responses to a 1% uniform sector shock. Figure 9 compares these results with

the baseline IRF from the full empirically estimated autoregressive matrix. The figure highlights the step-by-step increase in inflation persistence due to sector heterogeneity. In the first scenario, where both spillovers and heterogeneity are eliminated, aggregate inflation rises by 1% but rapidly decays to 0.38% by the end of the first quarter, with a half-life of less than one quarter, and the impact nearly vanishes by year-end.

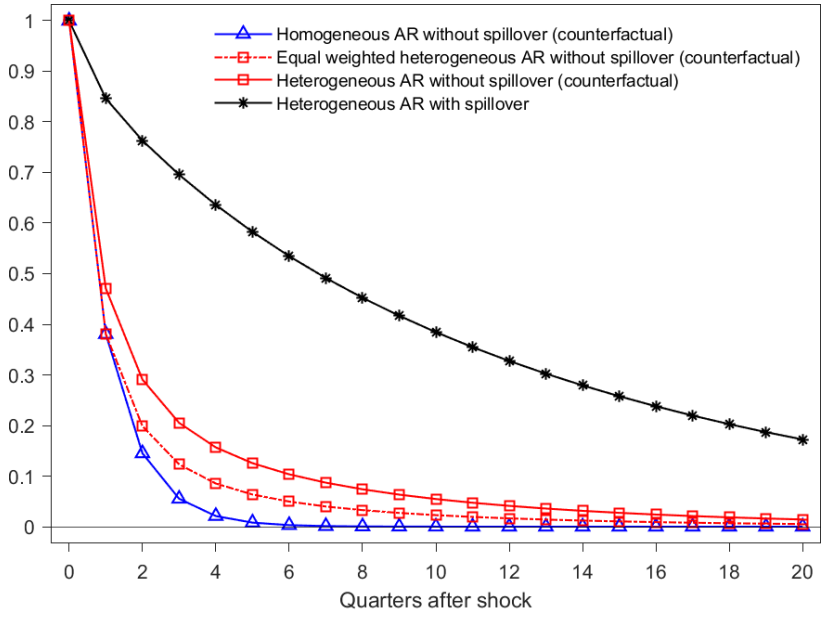


Figure 9: Aggregate Impulse Responses to Uniform Sectoral Shocks

Notes: This figure conducts three counterfactual exercises and presents three hypothetical impulse responses of aggregate inflation to uniform 1% inflation shocks across all sectors alongside the baseline IRFs (black line) for $h = 0, ..., 20$. The blue line marked with triangles eliminates heterogeneous sector self-persistence, heterogeneous consumption basket weight, and spillover effects. The red dash-dotted line marked with squares allows for heterogeneous sector self-persistence but eliminates heterogeneous consumption basket weight and spillover effects. The red solid line marked with squares allows for heterogeneous sector self-persistence and heterogeneous consumption basket weight but eliminates spillover effects.

In the second scenario, where heterogeneous sector self-persistence is introduced but basket weights remain equal, the IRF shifts marginally. The initial 1% rise still declines to 0.38% by the end of the first quarter, but the persistence increases slightly due to the presence of more persistent sectors. The decay of inflation slows down, extending the tail of the IRF. In the third scenario, where both sectoral heterogeneity in self-persistence and consumption basket weight are introduced, inflation persistence rises further. The half-life of the shock extends to approximately one quarter, and the IRF shows a slightly fatter tail. This amplification is a direct consequence of the positive relationship between basket weight and persistence, as illustrated in Figure 8.

However, none of these heterogeneity effects is comparable to the persistence generated by sectoral spillovers, as discussed in the previous section. The baseline IRF, shown by the

black line, exhibits significantly greater and more prolonged inflation persistence. Inflation drops only to 0.85% in the first quarter following the shocks and remains above 0.5% until the seventh quarter. Furthermore, the long-term impact is substantial, with inflation still elevated at 17 bps even five years after the initial shock.

These results underscore the pivotal role of sectoral spillovers in sustaining and amplifying inflationary pressures within the economy. Policymakers must carefully consider the potential for spillovers when formulating inflation-targeting strategies. A deeper understanding of these intersectoral dynamics can lead to more effective interventions, helping to mitigate the risk of persistent inflation.

Sectoral Heterogeneity and Relative Contribution of Sector Inflation. How does sector heterogeneity change the relative importance of sectors? Figure 7 makes the case that the top 5 sectors account for 81% aggregate inflation. In the simplest case when there are no sector spillovers and no sector heterogeneity in self-persistence and basket weight, each of the sixteen sectors will contribute equally 6.25% to the inflation and its persistence. To understand the role of sector heterogeneity in changing the relative importance of sectors. We consider in Table 2 two intermediate cases between Figure 7 and the simplest case.

The table reports the relative contribution of the top 5 sectors (the percentage written in parenthesis is the assigned consumption basket share) and the Herfindahl-Hirschman Index (HHI) to the infinite sum of inflation. In the simplest case, the top five sectors would account for 31.25% and the HHI is 5.8%. We then consider the intermediate case with equal basket weight and no sector spillover. In this case, each sector's basket weight is 6.25% and the uneven contribution is coming from different sectors' persistence. We can see that most of the sectors contribute to total inflation roughly in the range of 6%. There are three sectors that stand out, "Housing and utilities", "Recreational goods and vehicles" and "Health care" because they have relatively more persistent inflation. Their contribution to the total inflation is 24%, 12%, and 9%, respectively. In this case, we observe the top five sectors account for 58% of the total inflation and have an HHI of 10.5%. This indicates heterogeneous persistence increases the inflation contribution of some sectors and increases the inflation share concentration.

In the second intermediate case, which is reported in Column (3), we consider equal basket weight but with sector spillover. We can compare Column (2) with Column (3) to see the importance of the spillover effect. With the sector spillover considered, there are notable increases in contribution for the high spillover sector, such as "Health care" from 9% to 21% and "Recreational goods and vehicles" from 12% to 19%. At the same time, we observe that the top five sectors account for a high 79% of the total inflation and a HHI of 15.7%.

When we compare Column (3) with Column (4), which is the full case in Figure 7, we

Table 2: Relative Sector Contribution: Top 5 Share and Herfindahl - Hirschman Index

	Simple case (1)	Equal basket weight and no sector spillover (2)	Equal basket weight with sector spillover (3)	Full case (4)
Top 5 sectors & shares		Housing (6.25%): 24% Rec. Goods (6.25%): 12% Health (6.25%): 9% Other Dur. (6.25%): 8% Food Bev. (6.25%): 5%	Housing (6.25%): 23% Health (6.25%): 21% Rec. Goods (6.25%): 19% Other Serv. (6.25%): 8% Food Serv. (6.25%): 8%	Housing (18%): 32% Health (12%): 21% Rec. Goods (3%): 16% Other Serv. (8%): 9% Food Serv. (6%): 7%
Top 5 total share	31.25%	58%	79%	81%
HHI	5.8%	10.5%	15.7%	18.7%

Notes: This table presents the relative contributions of each top 5 sector, the total contribution of the top 5 sectors, and the HHI to the infinite sum of aggregate IRFs to a uniform of 1% shocks in all sectors. HHI stands for Herfindahl-Hirschman Index. The percentage written in parentheses is the assigned consumption basket weight. Column (1) refers to the simple case with no heterogeneous sector self-persistence, no sector spillover, and equal basket weight. Each of the sixteen sectors will contribute equally 6.25% to the inflation persistence. Column (2) allows for heterogeneous sector self-persistence. Column (3) allows for heterogeneous sector self-persistence and basket weight. The full case allows for heterogeneous sector self-persistence, basket weight, and sector spillover.

can see the change in the contribution of equal basket weights to BEA basket weights in the presence of spillover. Some sectors, most notably the "Housing and utilities" sector, are becoming more important because of the basket weight gain. The top 5 total share and HHI further increase to 81% and 18.7%. In summary, our findings highlight that sectoral heterogeneity plays a meaningful role in drawing greater attention to certain systematically important sectors. While these contributions are important, the spillover effects we emphasized in the previous section emerge as a more significant driver, amplifying the overall impact across sectors.

7 Inflation Persistence Implication of Common Factors

In this subsection, we analyze the implications of common factors. We show that the common factor is very transitory and highly correlated with oil price changes. Most importantly, we illustrate common factor shock implies a fairly transitory inflation.

7.1 Common Factors and Crude Oil Price Changes

Based on the procedure represented by Miao et al. (2023) in detailed Eq.(A1), our model strongly suggests the use of a one-factor model. The estimated common factor exhibits

a strong correlation with changes in crude oil prices, as depicted in Figure 10. The time series of the estimated common factor and Brent crude oil price changes show a correlation of 0.47 over the whole sample from 1960Q2 to 2023Q3. This correlation is notably higher during periods of high inflation, reaching 0.54 during the Great Inflation era (from 1970Q1 to 1985Q4) and 0.78 during the COVID-19 pandemic (from 2021Q1 to 2023Q3). Hence, it is likely that the estimated common factor predominantly captures movements in oil price changes.[4] Crude oil price shocks not only affect production costs, but also affect household and firm expectations of future inflation, and thus have effects on aggregate inflation (Coibion and Gorodnichenko, 2015; Känzig, 2021). Our finding is also in line with Gagliardone and Gertler (2023), which shows that the oil price shock, in addition to monetary policy easing, played an important role in the post-COVID inflation surge before 2023.

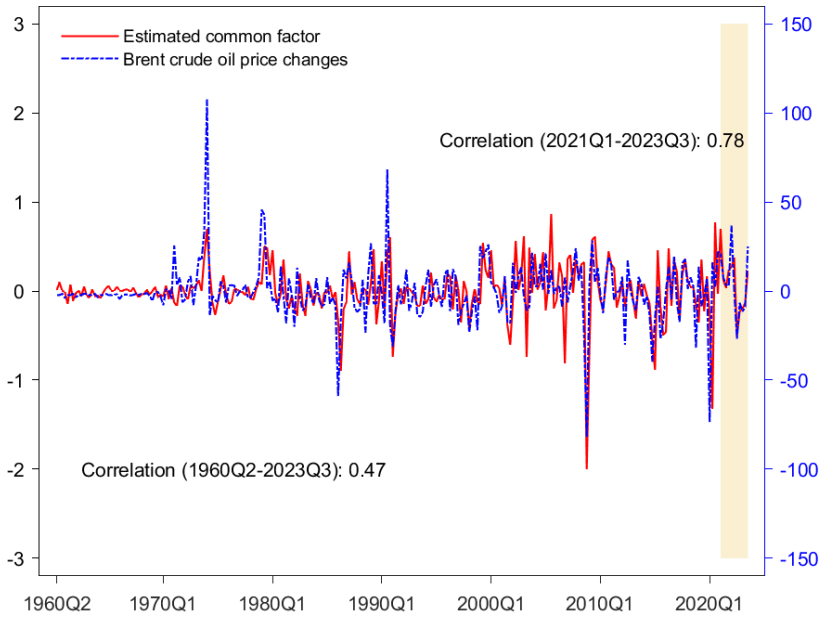


Figure 10: Common Factors and Brent Crude Oil Price Changes

Notes: This figure presents the time series of the estimated common factor $\widehat{f}_t$ (red solid line) and Brent crude oil price changes (blue dash-dotted line, available only from 1960Q2 onward) from 1960Q2 to 2023Q3. Brent crude oil price changes are demeaned because the common factor is estimated by our model using the demeaned time series.

[4]This relationship is further supported by the observation that gasoline prices are highly responsive to the common factor, as evidenced by the high factor loading of the gasoline sector. Additionally, this insight helps explain the previous surprising finding of the relatively low sectoral spillover from the gasoline sector, as oil price changes are primarily captured by the common factor, influencing all sectoral inflations with varying exposures.

7.2 Persistence in the Common Factor

As in Miao et al. (2023) and Foerster et al. (2011), we directly estimate the realized time series of the common factor. If we estimate the AR(1) model, i.e., $f_t = \rho f_{t-1} + \epsilon_t$ to measure the persistence in the common factor, the estimation yields $\widehat{\rho} = 0.025$, which is economically and statistically insignificant.[5] Zero lag is also the optimal lag chosen by the BIC, reported in Appendix H. This implies that the common factor itself tends to be transitory, and thus the persistence in the common factor itself could not account for the persistence in the post-COVID inflation hike. However, it is important to note that a temporary common shock impacting all sectors, albeit with varying exposures, can potentially exert a persistent influence on aggregate inflation through inter-sectoral propagation.

7.3 Aggregate Impulse Responses to Common Shock

After discussing the empirical characteristics of the common shock, we now turn our attention to analyzing its implications for inflation persistence. In this context, the black line in Figure 11 illustrates the aggregate inflation impulse response following a 1% common shock. The IRF suggests that the inflationary response to this shock is relatively short-lived, showing a fairly transitory pattern. Specifically, the half-life of the shock is approximately 0.75 quarters. However, it is important to note that while the initial effect of the shock wanes over time, its longer-term effects are still apparent. This is demonstrated by the impulse response of aggregate inflation, which, five years after the initial shock, remains elevated by 5 bps, indicating that the influence of common shocks endures, albeit at a much lower level.

To show how sectoral heterogeneity and inter-sectoral spillover shape the dynamic impact of common shocks on aggregate inflation persistence, we conduct two similar counterfactual exercises as in Figure 9 and compute the corresponding hypothetical IRFs upon 1% increase in the common shock. The first experiment, labeled as "heterogeneous autoregressive without spillover", removes inter-sectoral spillovers by setting off-diagonal elements of the autoregressive matrix $\widehat{\mathbf{A}}_1$ to zero in computing the IRF. This experiment focuses on how sectoral heterogeneity alone affects inflation persistence after a common shock. While in the second experiment, labeled as "homogeneous autoregressive without spillover", both spillovers and heterogeneity in sectoral own persistence are eliminated by using an average scalar equal to the average of the diagonal elements of $\widehat{\mathbf{A}}_1$.

Upon the 1% common shock, the two counterfactual IRFs exhibit very low persistence, and both decline quickly to zero within a year. This comparison highlights the importance of

[5]Note here we estimate the common factor first by using the FAVAR model and then fit it with an AR(1) model. However, this two-step approach still delivers a consistent estimate of the autoregressive coefficient of the common factor.

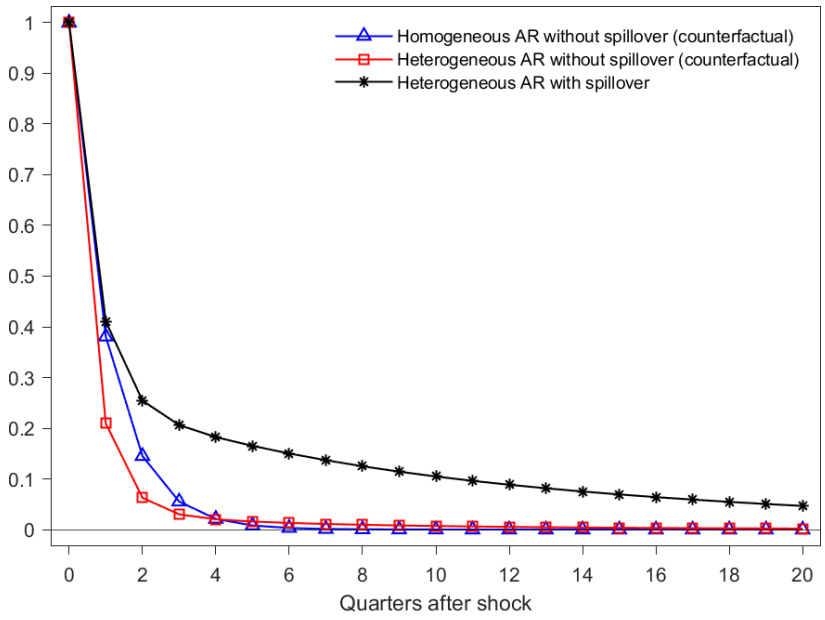


Figure 11: Aggregate Impulse Responses to Common Shock

Notes: This figure conducts two counterfactual exercises and presents two hypothetical impulse responses of aggregate inflation to 1% common shock alongside the baseline IRFs (black line) for $h = 1, ..., 20$. The blue line marked with triangles eliminates heterogeneous sector self-persistence and spillover effects. The red line marked with squares allows for heterogeneous sector self-persistence but eliminates spillover effects.

inter-sectoral spillover in making aggregate inflation more persistent upon common shocks. However, it also indicates that the role of sectoral heterogeneity in their own persistence is very limited for the persistence of aggregate inflation.

Note that the IRF of aggregate inflation is much more persistent upon 1% uniform sectoral shocks (half-life of 7 quarters) than the corresponding IRF upon the 1% common shock (half-life of 0.75 quarters), by comparing the black lines with asterisks in Figure 9 and Figure 11. This is simply because the factor loadings for the common factor vary across sectors, with the highest value for the gasoline sector, which has very low sectoral persistence. Meanwhile, the factor loadings for many other sectors have relatively small values. To better illustrate this, we quantify each sector's contribution to aggregate persistence upon common shocks.

Figure 12 breaks down the black line in Figure 11 to show the contribution of each sector to aggregate inflation persistence for $h = 0, ..., 20$, upon the common shock. The sectoral contributions to aggregate inflation persistence following common shocks exhibit distinct temporal patterns. In the first three months after a common shock, the "Gasoline and other energy goods" sector contributes the most, accounting for a maximum of 77% of the inflation. However, this energy-driven inflation declines sharply, reaching only 0.2% of its original size after four quarters. The remaining persistence of aggregate inflation is primarily driven by the "Housing and utilities" sector (yellow bars), whose contribution remains steady at around

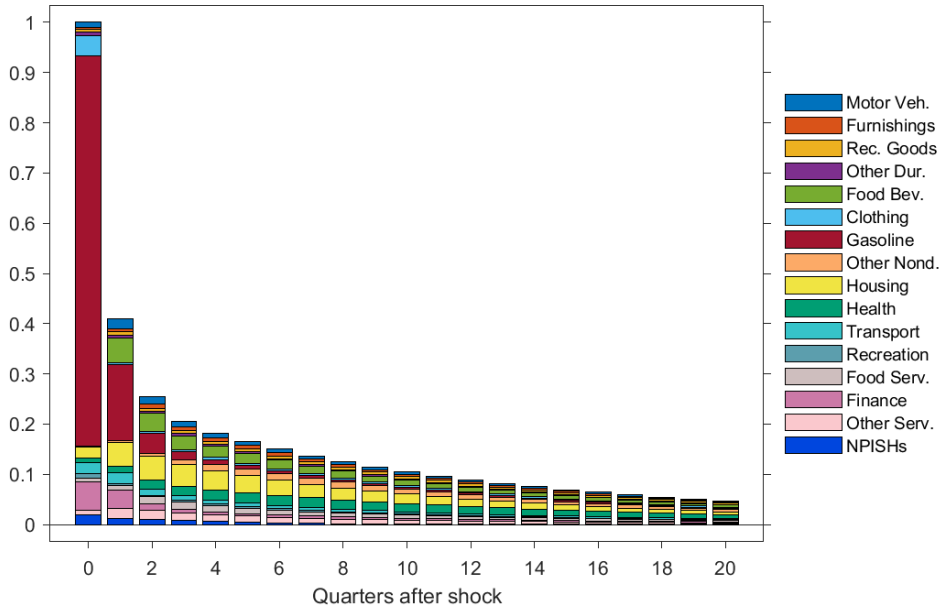


Figure 12: Sectoral Contribution to Aggregate Inflation Persistence

Notes: This figure presents the breakdown of aggregate inflation persistence on 1% common shock into 16 sectors for $h = 0, ..., 20$. The y-axis represents the level of contributions from each sector.

one-fifth between six months and three years after the shock, making it the top contributor during this period. After three years, however, the "Health care" sector surpasses "Housing and utilities" as the leading contributor, with its contribution rate increasing over time to reach 18% by the fifth year. Unlike the "Housing and utilities" sector, which relies mainly on its strong internal persistence, the "Health care" sector's contribution to aggregate inflation persistence is significantly influenced by sectoral spillover effects.

In previous sections, we conduct counterfactual experiments to evaluate the role of intersectoral spillover and sectoral heterogeneity in aggregate inflation persistence. An alternative approach is to estimate restrictive models without those features and compare the corresponding IRFs to sectoral and common shocks. In the Appendix I, we estimate two alternative models. The first restrictive model shuts down spillovers while allowing heterogeneous sectoral persistence, and the second assumes homogeneous sectoral persistence with no spillovers. Both models exhibit significantly lower inflation persistence compared to our general model, particularly in response to sectoral shocks.

8 Accounting for the Post-COVID-19 Period Inflation

The analysis above highlights the different implications of sector and common shocks for inflation, and three channels that affect inflation persistence. This section explores how

these shocks have influenced historical inflation, both with the full sample starting from the 1960s and focusing on the post-COVID-19 period. Our findings reveal that sectoral shocks have played a substantial role in the post-COVID-19 era, leading to higher and more persistent inflation due to their spillover effects. We also conduct prediction exercises and show our model generates more persistent and accurate out-of-sample forecasts than professional forecasters.

8.1 Decomposition of Aggregate Inflation

Using the moving average representation of the FAVAR model, the aggregate inflation can be decomposed into three parts:

$$\begin{aligned}\pi_t = \mathbf{w}'\mathbf{Y}_t &= \mathbf{w}' \sum_{s=0}^{\infty} (\mathbf{A}_1)^s \, \mathbf{\Lambda} f_{t-s} + \mathbf{w}' \sum_{s=0}^{\infty} (\mathbf{A}_1)^s \, \mathbf{u}_{t-s} \\ &= \mathbf{w}' (\mathbf{A}_1)^t \, \mathbf{Y}_0 + \underbrace{\mathbf{w}' \sum_{s=0}^{t-1} (\mathbf{A}_1)^s \, \mathbf{\Lambda} f_{t-s}}_{common\ shock\ component} + \underbrace{\mathbf{w}' \sum_{s=0}^{t-1} (\mathbf{A}_1)^s \, \mathbf{u}_{t-s}}_{sectoral\ shock\ component} .\end{aligned} \tag{12}$$

Eq.(12) consists of starting inflation, the past and current common shock component associated with the common factors and factor loading, and the past and current sectoral shock component connected to the sectoral shocks. The effect of the first term $\mathbf{w}' (\mathbf{A}_1)^t \mathbf{Y}_0$ is negligible after 1970 because it shrinks to zero quickly as t increases.

Figure 13 shows the aggregate inflation, π_t versus its common shock component - the second term of the right-most expression of Eq.(12). The aggregate inflation and common shock component have a relatively strong association (0.6 for 1970Q1-2023Q3), indicating the necessity of the inclusion of a common factor in the VAR model. Meanwhile, aggregate inflation is noticeably more volatile than the common shock component during high inflation periods, i.e., the Great Inflation period and the post-COVID period, indicating the relative rise in the contribution of sectoral shock components to aggregate inflation.

8.2 Sources of Aggregate Inflation in Post-COVID-19 Period

Using the decomposition method in Eq.(12), we explore the sources of the post-COVID inflation hike. Figure 14 shows the breakdown of aggregate inflation into the sectoral (red bars) and common shock (blue bars) components in the post-COVID period.

In the figure, we report the demeaned QoQ inflation. Initially, during 2020Q1 and 2020Q2, aggregate inflation experienced a significant decline, predominantly driven by com-

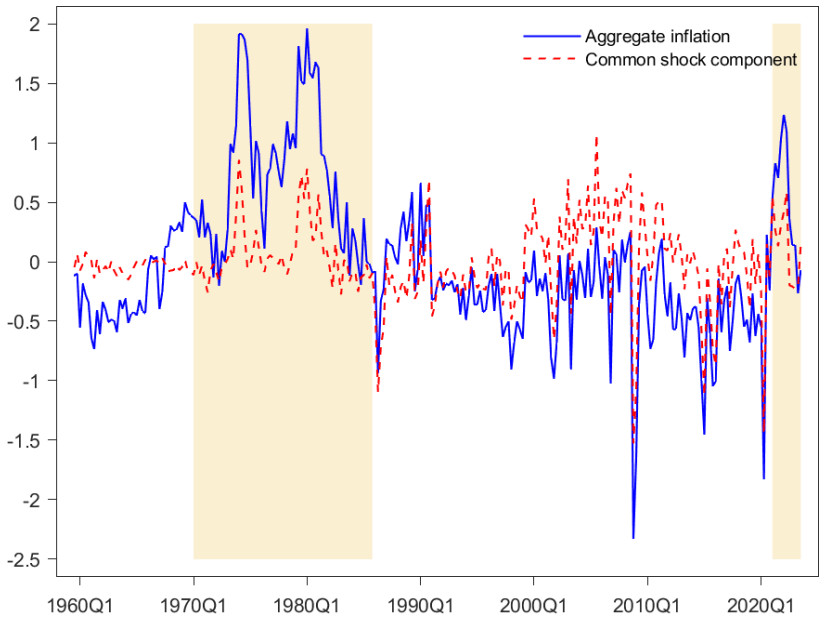


Figure 13: Aggregate Inflation and Common Shock Component

Notes: This figure presents the time series of the demanded quarter-on-quarter aggregate inflation (blue solid line) and its common shock component (red dash-dotted line) — the second term of the right-most expression of Eq.(12) for the whole sample period.

mon shocks. This period was marked by the outbreak of COVID-19, which led to widespread lockdowns and a severe reduction in economic activity globally. Additionally, the crude oil price slump during this time, induced by a combination of reduced demand from the pandemic and an oil price war between major producers, exacerbated the decline in inflation.

As the economy began to recover in 2020Q3, we observed a substantial rebound in inflation. A significant rise was particularly evident after 2021Q2, driven by sectoral shocks that heavily influenced the inflation surge. To formally analyze this, we conduct a variance decomposition to understand the contribution of the common factor to inflation.

$$\textbf{Common factor share} = \text{var}(\underbrace{\mathbf{w}' \sum_{s=0}^{t-1} (\mathbf{A}_1)^s \, \mathbf{\Lambda} f_{t-s}}_{\textit{common shock component}}) / \text{var}(\pi_t). \tag{13}$$

Between 2021Q1 and 2023Q3, the common factor accounted for 56% of the variation in inflation, while sectoral shocks contributed the remaining 44%. By contrast, during the relatively low-inflation period of 2010-2019, the common factor explained 84% of the variation, indicating a markedly higher share of sectoral shocks in the post-COVID period compared to the previous decade. Given the stark difference in inflation persistence between common shocks and sectoral shocks, drawing conclusions about inflation persistence based on the 2010-2019 period would overlook the critical role of sectoral contributions observed in recent years.

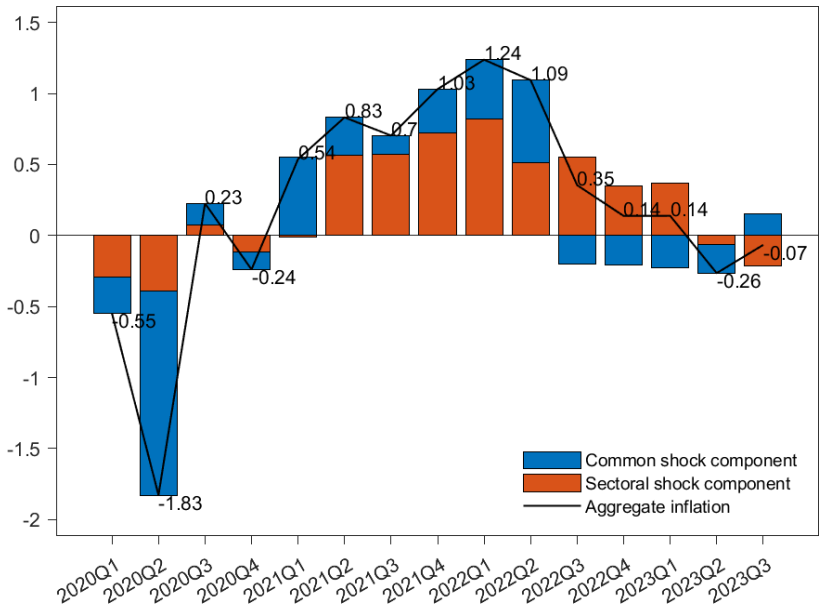


Figure 14: Decomposition of Aggregate Inflation: Post-COVID-19 Period

Notes: This figure presents the breakdown of the demeaned quarter-on-quarter aggregate inflation (black line) into the sectoral component (red bars) and common shock component (blue bars) in the post-COVID period from 2020Q1 to 2023Q3. The numbers on the black line represent the demeaned quarter-on-quarter aggregate inflation.

Figure 15 further decomposes the sectoral shock component into the 16 sectors and reveals that "Motor vehicles and parts", "Furnishings and durable household equipment", "Gasoline and other energy goods", and "Housing and utilities" were among the most influential in driving inflation. The "Motor vehicles and parts" sector particularly impacted inflation throughout the 2021Q2-2022Q2 due to severe production bottlenecks caused by the global semiconductor shortage and supply chain disruptions (Datta et al., 2022). Similarly, the "Food and beverages purchased for the off-premises consumption" sector contributed steadily to inflation throughout the period, with marked price increases in early 2022 driven by the pandemic-induced shift toward more at-home dining and persistent supply chain challenges.

Energy prices, particularly gasoline, surged notably in the latter half of 2021 and early 2022 due to the outbreak of the Russia-Ukrane war and the recovery in travel and transportation demand combined with ongoing supply constraints (Kilian and Zhou, 2022). The "Furnishings and durable household equipment" sector saw substantial price increases during the second half of 2021, driven by heightened consumer demand for home improvement and persistent supply chain issues. Additionally, rising housing costs and utility prices were particularly impactful during 2021Q4 and 2023Q1, as increased demand for housing and supply limitations drove significant price increases (Glaeser et al., 2021).

These sector-specific dynamics underscore the multifaceted nature of inflation during this

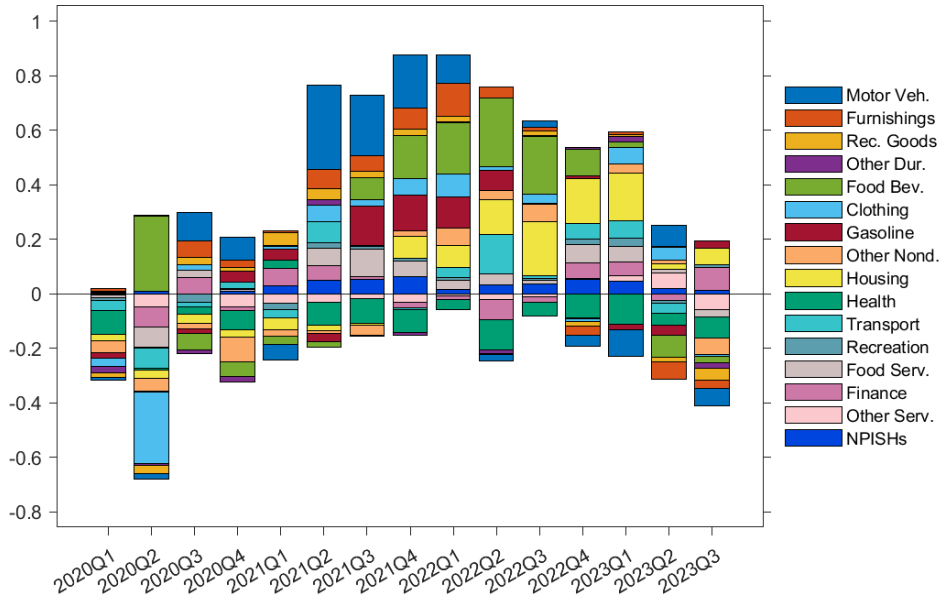


Figure 15: Decomposition of Sectoral Shock Component: Post-COVID-19 Period

Notes: This figure presents the decomposition of the sectoral shock component into 16 distinct sectors in the post-COVID period from 2020Q1 to 2023Q3.

period, influenced by a combination of supply chain disruptions, shifts in consumer demand, and broader economic recovery trends. Moreover, sectoral shocks spill over to other sectors through the spillover network, and thus, their effects do not simply average out.

Returning to Figure 14, we observe a gradual decline in aggregate inflation from 2022Q3 onwards, with a notable dip in 2023Q2. This decline can be primarily attributed to a reduction in common shocks, which aligns with the Federal Reserve's deliberate tightening of monetary policy to curb high and persistent inflation. Beginning in March 2022, the Fed implemented a series of interest rate hikes, raising the federal funds rate from near zero to over 5% by mid-2023, and also reduced its balance sheet through quantitative tightening.

Moreover, as we have discussed above, a significant component of the common shocks is associated with crude oil prices, which have experienced a notable decline since the middle of 2022. This decline can be attributed to a combination of factors, including increased production from major oil-producing countries, a slowdown in global economic activity, and the effects of tighter monetary policy reducing overall demand. The reduction in crude oil prices lowered energy costs throughout the economy, reducing transportation and production costs across various sectors, thereby playing a pivotal role in tempering overall inflation rates.

Interestingly, while the common shock component experienced a significant decline, sectoral shocks remained relatively persistent, particularly in the food and housing sectors, which were still affected by ongoing supply chain disruptions, labor shortages, and other logistical challenges. This sectoral persistence prevented aggregate inflation from returning

to its average level, highlighting the importance of sector-specific factors in driving aggregate inflation dynamics.

In summary, this decomposition analysis of aggregate inflation underscores the dynamic interplay between common and sectoral shocks in driving inflation trends during the post-COVID period. Our study highlights the pivotal role of sectoral shocks in driving the peak inflation phase and their persistent nature, even as aggregate inflation subsequently declined due to the decrease in the common shock component. The findings suggest that policymakers should consider both aggregate and sector-specific factors when addressing inflationary pressures, as the persistence of sectoral shocks can hinder the effectiveness of monetary policy in stabilizing overall price levels.

8.3 Counterfactual Experiments

To quantify the impact of sectoral spillover and sectoral heterogeneity in persistence on aggregate inflation, we conduct two counterfactual experiments by simulating the hypothetical aggregate inflation under conditions where sectoral spillover or both sectoral spillover and sectoral heterogeneity are eliminated, while holding other parameters and shocks constant. Specifically, for the first experiment, we construct a counterfactual autoregressive coefficient matrix, denoted as $\widehat{\mathbf{A}}_1^c$ and labeled as "heterogeneous autoregressive without spillover", by setting the off-diagonal entries of the estimated matrix $\widehat{\mathbf{A}}_1$ to zero, thereby retaining only the original diagonal coefficients. This adjustment effectively disables the sectoral spillover channel, isolating its influence from the model. For the second experiment, we shut down both sectoral spillover and sectoral heterogeneity and use the average of the diagonal of the estimated matrix $\widehat{\mathbf{A}}_1$ to construct another counterfactual autoregressive coefficient scalar $\widehat{a}_1^c$, denoted as "homogeneous autoregressive without spillover". Utilizing the estimated shocks and factor loading ($\widehat{f}_t$, $\widehat{\mathbf{u}}_t$, and $\widehat{\mathbf{\Lambda}}$), along with the modified autoregressive matrix/scalar (matrix $\widehat{\mathbf{A}}_1^c$ or scalar $\widehat{a}_1^c$), we compute the two counterfactual time series data for aggregate inflation using the following formula:

$$\widehat{\pi}_t^{c1} = \mathbf{w}'\widehat{\mathbf{Y}}_t^{c1} = \mathbf{w}'\left(\widehat{\mathbf{A}}_1^c\right)^t \mathbf{Y}_0 + \mathbf{w}'\sum_{s=0}^{t-1}\left(\widehat{\mathbf{A}}_1^c\right)^s \widehat{\mathbf{\Lambda}}\widehat{f}_{t-s} + \mathbf{w}'\sum_{s=0}^{t-1}\left(\widehat{\mathbf{A}}_1^c\right)^s \widehat{\mathbf{u}}_{t-s}$$

$$\widehat{\pi}_t^{c2} = \mathbf{w}'\widehat{\mathbf{Y}}_t^{c2} = \mathbf{w}'\left(\widehat{a}_1^c\right)^t \mathbf{Y}_0 + \mathbf{w}'\sum_{s=0}^{t-1}\left(\widehat{a}_1^c\right)^s \widehat{\mathbf{\Lambda}}\widehat{f}_{t-s} + \mathbf{w}'\sum_{s=0}^{t-1}\left(\widehat{a}_1^c\right)^s \widehat{\mathbf{u}}_{t-s}.$$

Figure 16 illustrates the comparison between the demeaned actual QoQ aggregate inflation and the two counterfactual counterparts for the whole sample period. It is important to note that sectoral spillovers tend to amplify both common and sectoral shocks during

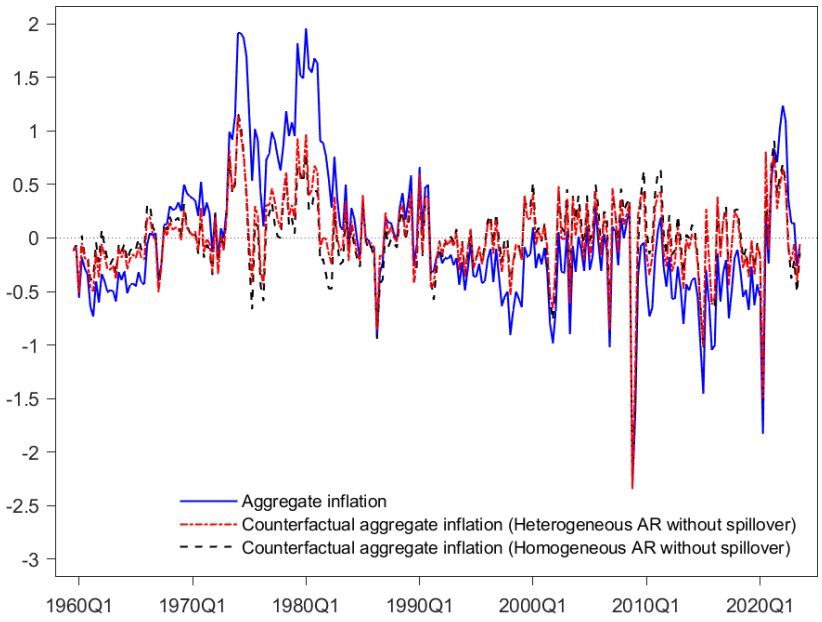


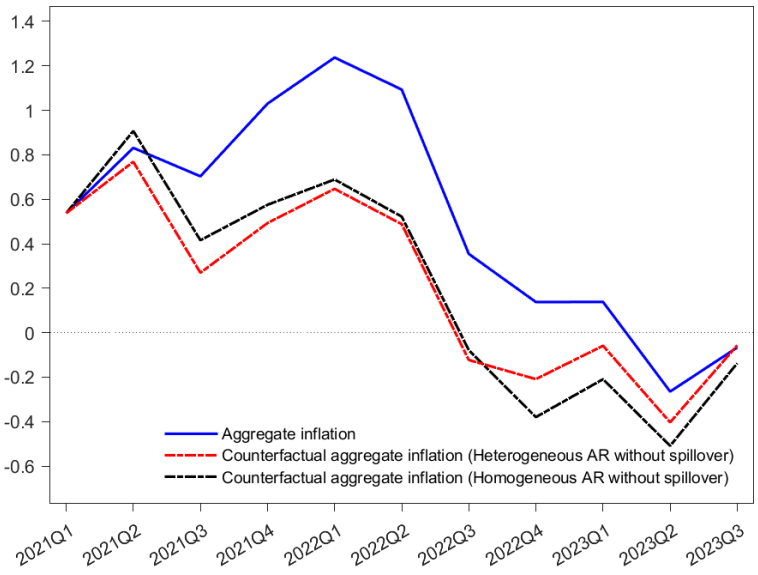
Figure 16: Aggregate Inflation with and without Spillover

Notes: This figure presents the actual demeaned quarter-on-quarter aggregate inflation (blue solid line) and two counterfactual counterparts for the whole sample period. The black dashed line eliminates heterogeneous sector self-persistence and spillover effects. The red dash-dotted line allows for heterogeneous sector self-persistence but eliminates spillover effects.

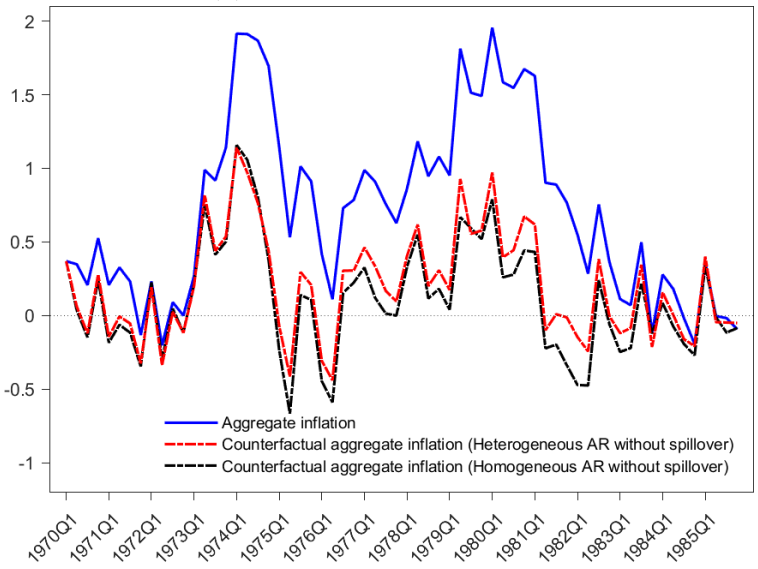
high inflation episodes, such as the Great Inflation of the 1970s and early 1980s, as well as the post-COVID inflation surge. Consequently, it is unsurprising that the two counterfactual inflation consistently underestimate the actual inflation rate during these periods. In contrast, the two counterfactual inflation rates closely approximate actual inflation levels observed during the low inflation period spanning from the late 1980s to 2020. Moreover, aggregate inflation patterns in the two counterfactuals are quite similar, indicating that sectoral heterogeneity contributes little to inflation persistence.

In Figure 17, we zoom in on two distinct high inflation episodes: the post-COVID period (2021Q1-2023Q3) and the Great Inflation period (1970Q1-1985Q4). Both subfigures demonstrate that eliminating sectoral spillovers would substantially dampen aggregate inflation during these periods, while sectoral heterogeneity does only slightly contribute.

Figure 17(a) examines recent inflation dynamics, illustrating that shutting down sectoral spillovers would have, on average, lowered quarterly aggregate inflation by 0.3 log points, representing a substantial 22% reduction from 2021Q1 to 2023Q3, as shown in Table 3. The largest observed gap between counterfactual (heterogeneous autoregressive without spillover) and actual aggregate inflation was approximately 0.6 log points in 2022Q1 and Q2, coinciding with the peak inflation rate. Moreover, shutting down sectoral spillovers, aggregate inflation would have reverted to the mean three quarters earlier, that is 2022Q3, instead of 2023Q2



(a) Post-COVID-19 Period



(b) Great Inflation Period

Figure 17: Aggregate Inflation and Two Counterfactual Predictions in Post-COVID-19 Period and Great Inflation Period

Notes: This figure presents the actual demeaned quarter-on-quarter aggregate inflation (blue solid line) and two counterfactual counterparts in the post-COIVD period (2021Q1-2023Q3) and the Great Inflation period (1970Q1-1985Q4). The black dashed line eliminates heterogeneous sector self-persistence and spillover effects. The red dashed line allows for heterogeneous sector self-persistence but eliminates spillover effects.

as observed in the data, given the same shocks and parameters. This finding underscores the contribution of sectoral spillovers to the persistence of aggregate inflation. By contrast, on average further eliminating the sectoral heterogeneity in persistence does not alter the counterfactual results substantially, as shown in Table 3, indicating that sectoral heterogene-

ity contributes little to the persistence of post-COVID inflation. Only after 2022Q2, further eliminating the sectoral heterogeneity in persistence could further lower aggregate inflation, compared with the counterfactual prediction without spillover effects only.

Table 3: Average Reduction in Aggregate Inflation in Two Counterfactual Experiments

Counterfactual experiments	Post-COVID period (2021Q1-2023Q3)	Great inflation period (1970Q1-1985Q4)
Heterogenous AR without spillover	-22.13%	-34.02%
Homogenous AR without spillover	-22.01%	-39.94%

Notes: This table presents the average reduction from two counterfactual experiments compared to the actual demeaned quarter-on-quarter aggregate inflation in the post-COVID period and the Great Inflation period. The average reduction is calculated by dividing the mean difference between counterfactual inflation and aggregate inflation by the mean of aggregate inflation for the given sample period.

In Figure 17(b), focusing on the Great Inflation period, we observe that eliminating sectoral spillover effects would have reduced average quarterly aggregate inflation by 0.52 log points, equivalent to a notable 34% decline in the inflation rate, as shown in Table 3. Notably, the largest discrepancy between counterfactual prediction without spillover only and actual aggregate inflation, reaching 1.26 log points, occurred in 1974Q4. Meanwhile, aggregate inflation patterns in the two counterfactual predictions are largely similar, but the gap tends to be slightly larger between 1975 and 1983. As shown in Table 3, shutting down both the sectoral heterogeneity in persistence and spillover would have reduced the aggregate inflation by 40% on average during the Great Inflation period, indicating that sectoral heterogeneity may play a more important role than its role in post-COVID inflation.

In summary, this quantitative exercise underscores the critical role of sectoral spillover in amplifying and propagating temporary sectoral and common shocks, thereby enhancing the persistence of aggregate inflation during high inflation episodes.[6] By contrast, sectoral heterogeneity in persistence contributes little to post-COVID inflation but slightly more to the Great Inflation period.

8.4 Out-of-sample Inflation Forecast

Is the inflation observed since 2021 transitory or relatively persistent? To address this question, we re-estimate the model parameters using data only up to 2019Q4. Based on this re-estimation, we generate out-of-sample inflation forecasts by incorporating realized sector-specific and common shocks for each quarter from 2021 to 2023. The model-implied forecast values are presented in Figure 18.

[6]Appendix K shows that the counterfactual results are robust if the number of common factors is set to two.

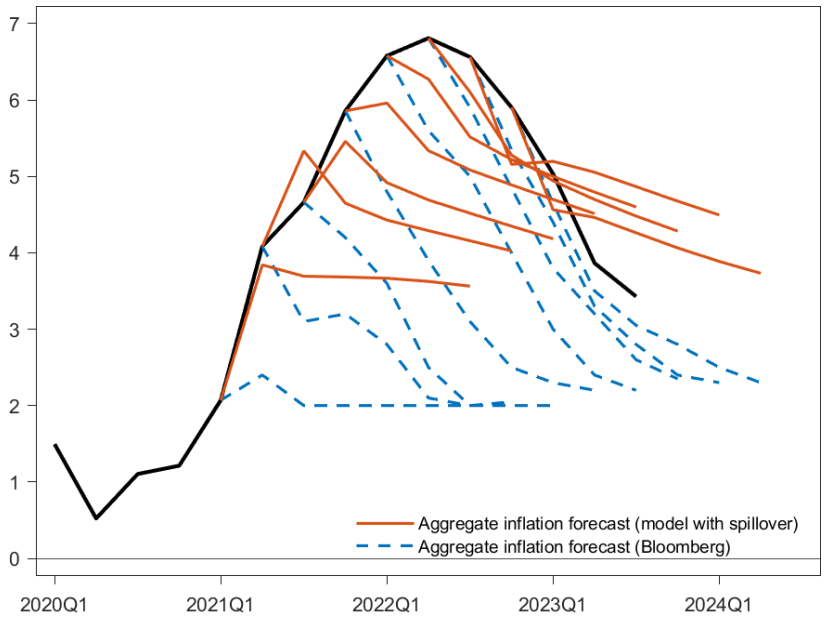


Figure 18: Out-of-Sample Inflation Forecasts

Notes: This figure presents the out-of-sample inflation forecasts from 2021Q1 to 2022Q4, with each forecast extending over 6 quarters. The black solid line represents the realized PCE inflation, while the orange solid lines represent the out-of-sample inflation forecasts generated by our model, and the blue dashed lines represent the inflation forecasts provided by Bloomberg.

In Figure 18, the black line represents realized PCE inflation, while the blue lines depict the median 6-quarter-ahead inflation forecasts from the Bloomberg survey. Notably, in 2021, financial market participants largely anticipated a return to the 2% inflation target within a year. However, in 2022 and 2023, these expectations shifted, with participants forecasting that inflation would take approximately two years to return to the target level.

In contrast, the orange lines represent the out-of-sample inflation forecasts generated by our model. Our results indicate that, during 2021 and most of 2022, the model predicted inflation to be significantly more persistent than the forecasts of financial participants. Specifically, the model projected inflation to remain around the 3-4% level two years from the initial forecast points. By 2022Q4 — the final quarter in our forecast horizon — the model predicted inflation would decline to approximately 3% after two years. These projections align closely with the inflation trajectory observed, suggesting that our model provides more realistic out-of-sample predictions compared to the expectations of financial participants.

9 Conclusion

This paper highlights the critical role of sectoral shocks and intersectoral spillovers in driving aggregate inflation persistence, particularly in the post-COVID period. We provide a unified

framework to disentangle the contributions of common factors, sectoral heterogeneity, and intersectoral spillovers. This approach offers a flexible, data-driven methodology for real-time policy analysis. Our findings reveal that spillovers are the dominant force sustaining inflation persistence. These insights are crucial for policymakers to combat persistent inflationary pressures in an interconnected economy with recurrent sector-specific disruptions.

References

Acemoglu, D., U. Akcigit, and W. Kerr (2016). Networks and the macroeconomy: An empirical exploration. *NBER Macro Annual 30*(1), 273–335.

Acemoglu, D., V. M. Carvalho, A. Ozdaglar, and A. Tahbaz-Salehi (2012). The network origins of aggregate fluctuations. *Econometrica 80*(5), 1977–2016.

Acharya, V. V., M. Crosignani, T. Eisert, and C. Eufinger (2023). How do supply shocks to inflation generalize? Evidence from the pandemic era in Europe. Working paper, National Bureau of Economic Research.

Afrouzi, H. and S. Bhattarai (2023). Inflation and GDP dynamics in production networks: A sufficient statistics approach. Working paper, National Bureau of Economic Research.

Afrouzi, H., S. Bhattarai, and E. Wu (2024). Relative-price changes as aggregate supply shocks revisited: Theory and evidence. *Journal of Monetary Economics 148*, 103650.

Altissimo, F., B. Mojon, and P. Zaffaroni (2009). Can aggregation explain the persistence of inflation? *Journal of Monetary Economics 56*(2), 231–241.

Angeletos, G.-M., C. Lian, and C. K. Wolf (2024). Deficits and inflation: HANK meets FTPL. Working paper, National Bureau of Economic Research.

Ascari, G., D. Bonam, and A. Smadu (2024). Global supply chain pressures, inflation, and implications for monetary policy. *Journal of International Money and Finance 142*, 103029.

Atalay, E. (2017). How important are sectoral shocks? *American Economic Journal: Macroeconomics 9*(4), 254–280.

Baqaee, D. R. and E. Farhi (2018). Macroeconomics with heterogeneous agents and input-output networks. Working paper, National Bureau of Economic Research.

Baqaee, D. R. and E. Farhi (2019). The macroeconomic impact of microeconomic shocks: Beyond Hulten's theorem. *Econometrica 87*(4), 1155–1203.

Baqaee, D. R. and E. Farhi (2020). Productivity and misallocation in general equilibrium. *The Quarterly Journal of Economics 135*(1), 105–163.

Barrot, J.-N. and J. Sauvagnat (2016). Input specificity and the propagation of idiosyncratic shocks in production networks. *The Quarterly Journal of Economics 131*(3), 1543–1592.

Beaudry, P., C. Hou, and F. Portier (2024). The dominant role of expectations and broad-based supply shocks in driving inflation. Forthcoming at NBER Macro Annual 2024.

Benigno, P. and G. B. Eggertsson (2023). It's baaack: The surge in inflation in the 2020s and the return of the non-linear Phillips curve. Working paper, National Bureau of Economic Research.

Bernanke, B. and O. Blanchard (2023). What caused the US pandemic-era inflation? In *Hutchins Center Working Papers*. The Brookings Institution.

Bianchi, F., R. Faccini, and L. Melosi (2023). A fiscal theory of persistent inflation. *The Quarterly Journal of Economics 138*(4), 2127–2179.

Borio, C. E., M. Lombardi, J. Yetman, and E. Zakrajšek (2023). *The two-regime view of inflation*. BIS, Bank for International Settlements.

Carvalho, V. and X. Gabaix (2013). The great diversification and its undoing. *American Economic Review 103*(5), 1697–1727.

Carvalho, V. M., M. Nirei, Y. U. Saito, and A. Tahbaz-Salehi (2021). Supply chain disruptions: Evidence from the great east Japan earthquake. *The Quarterly Journal of Economics 136*(2), 1255–1321.

Carvalho, V. M. and A. Tahbaz-Salehi (2019). Production networks: A primer. *Annual Review of Economics 11*(1), 635–663.

Cochrane, J. H. (2023). *The fiscal theory of the price level*. Princeton University Press.

Coibion, O. and Y. Gorodnichenko (2015). Is the Phillips curve alive and well after all? Inflation expectations and the missing disinflation. *American Economic Journal: Macroeconomics 7*(1), 197–232.

Comin, D. A., R. C. Johnson, and C. J. Jones (2023). Supply chain constraints and inflation. Working paper, National Bureau of Economic Research.

Datta, D. D., L. Feiveson, E. Peneva, and G. Rua (2022). Bottlenecks, shortages, and soaring prices in the US economy. FEDS Notes.

De Graeve, F. and J. D. Schneider (2023). Identifying sectoral shocks and their role in business cycles. *Journal of Monetary Economics 140*, 124–141.

Demirer, M., F. X. Diebold, L. Liu, and K. Yilmaz (2018). Estimating global bank network connectedness. *Journal of Applied Econometrics 33*(1), 1–15.

Ferrante, F., S. Graves, and M. Iacoviello (2023). The inflationary effects of sectoral reallocation. *Journal of Monetary Economics 140*, S64–S81.

Foerster, A. T., P.-D. G. Sarte, and M. W. Watson (2011). Sectoral versus aggregate shocks: A structural factor analysis of industrial production. *Journal of Political Economy 119*(1), 1–38.

Forni, M. and L. Reichlin (1998). Let's get real: A factor analytical approach to disaggregated business cycle dynamics. *The Review of Economic Studies 65*(3), 453–473.

Gabaix, X. (2011). The granular origins of aggregate fluctuations. *Econometrica 79*(3), 733–772.

Gagliardone, L. and M. Gertler (2023). Oil prices, monetary policy and inflation surges. Working paper, National Bureau of Economic Research.

Glaeser, E. L., J. Gyourko, and R. E. Saks (2021). Housing supply and affordability: Evidence from rents, housing consumption and household location. *Journal of Economic Perspectives 35*(1), 131–154.

Guerrieri, V., G. Lorenzoni, L. Straub, and I. Werning (2022). Macroeconomic implications of COVID-19: Can negative supply shocks cause demand shortages? *American Economic Review 112*(5), 1437–1474.

Hazell, J. and S. Hobler (2024). Do deficits cause inflation? A high frequency narrative approach. Working paper.

Känzig, D. R. (2021). The macroeconomic effects of oil supply news: Evidence from OPEC announcements. *American Economic Review 111*(4), 1092–1125.

Kilian, L. and X. Zhou (2022). The impact of rising oil prices on US inflation and inflation expectations in 2020–23. *Energy Economics 113*, 106228.

Kock, A. B. and L. Callot (2015). Oracle inequalities for high dimensional vector autoregressions. *Journal of Econometrics 186*(2), 325–344.

Lee, J. H., Z. Shi, and Z. Gao (2022). On LASSO for predictive regression. *Journal of Econometrics 229*(2), 322–349.

Li, N. and V. L. Martin (2019). Real sectoral spillovers: A dynamic factor analysis of the great recession. *Journal of Monetary Economics 107*, 77–95.

Long, J. B. and C. I. Plosser (1987). Sectoral vs. aggregate shocks in the business cycle. *American Economic Review 77*(2), 333–336.

Mayoral, L. (2013). Heterogeneous dynamics, aggregation, and the persistence of economic shocks. *International Economic Review 54*(4), 1295–1307.

Mayoral, L. and M. D. Gadea (2011). Aggregate real exchange rate persistence through the lens of sectoral data. *Journal of Monetary Economics 58*(3), 290–304.

Miao, K., P. C. Phillips, and L. Su (2023). High-dimensional VARs with common factors. *Journal of Econometrics 233*(1), 155–183.

Minton, R. and B. Wheaton (2023). Delayed inflation in supply chains: Theory and evidence. Available at SSRN 4470302.

Pesaran, M. H. and A. Chudik (2014). Aggregation in large dynamic panels. *Journal of Econometrics 178*, 273–285.

Rubbo, E. (2023). Networks, Phillips curves, and monetary policy. *Econometrica 91*(4), 1417–1455.

Su, L., Z. Shi, and P. C. B. Phillips (2016). Identifying latent structures in panel data. *Econometrica 84*(6), 2215–2264.

Tibshirani, R. (1996). Regression shrinkage and selection via the Lasso. *Journal of the Royal Statistical Society Series B: Statistical Methodology 58*(1), 267–288.

Zaffaroni, P. (2004). Contemporaneous aggregation of linear dynamic models in large economies. *Journal of Econometrics 120*(1), 75–102.

Online Appendix

Appendix Contents

A Estimation **47**

A.1 Estimation with Penalized Method 47

A.2 VAR Lag Selection 48

A.3 Normalization of the Factor Loadings and Common Factor 48

B Simulation **50**

C Estimated Autoregressive Matrix without Lasso **54**

D Ranking of Sectoral Inflation Persistence **55**

E Eigenvalues of the Estimated VAR Matrix **56**

F Procedure of Constructing Production I-O Matrix **57**

G Aggregate Inflation Impulse Responses to Each Sectoral Shock **58**

H Lag Selection for Estimated Common Factor Fitting AR Model **59**

I Alternative Approach to Evaluating Spillover **60**

J Sources of Aggregate Inflation in Great Inflation Period **63**

K Robustness of Counterfactual Results: Two Common Factors **65**

A Estimation

A.1 Estimation with Penalized Method

In our context, we have 256p (= 16 × 16 × number of lags) slope coefficients in the VAR system to be estimated from a balanced panel of 16 sectors and 258 time periods. We follow the notations in Section 3. The high-dimensional VAR model of order p with r common factors is expressed as:

$$\mathbf{Y}_t = \sum_{k=1}^{p} \mathbf{A}_k \mathbf{Y}_{t-k} + \mathbf{\Lambda} \mathbf{f}_t + \boldsymbol{\mu} + \mathbf{u}_t, \quad t = 1, 2 \ldots, T.$$

To get rid of the fixed effect $\boldsymbol{\mu}$, we carry out a within-group demeaning of the data for each individual i over the time dimension to obtain $\widetilde{\mathbf{Y}}$ and $\widetilde{\mathbf{X}}$. Recall that $\mathbf{B} = (\mathbf{A}_1, \ldots, \mathbf{A}_p)$ collects all the VAR slope coefficients.

The first-step estimator:

(a) Since $\mathbf{F}$ and $\mathbf{\Lambda}$ are together in a multiplicative form, we denote $\mathbf{\Psi} = \mathbf{\Lambda F}$, and will penalize it by the nuclear norm $\|\mathbf{\Psi}\|_* = \text{trace}(\sqrt{\mathbf{\Psi}'\mathbf{\Psi}})$. We preliminarily estimate $\mathbf{B}$ and $\mathbf{\Psi}$ by the following penalized regression:

$$\left(\widetilde{\mathbf{B}}, \widetilde{\mathbf{\Psi}}\right) = \underset{(\mathbf{B}, \mathbf{\Psi})}{\text{argmin}} \frac{1}{2NT} \left\| \widetilde{\mathbf{Y}} - \mathbf{B}\widetilde{\mathbf{X}} - \mathbf{\Psi} \right\|_{\mathcal{F}}^2 + \frac{\gamma_1}{N} \left| \text{vec}\left(\mathbf{B}\right) \right|_1 + \frac{\gamma_2}{\sqrt{NT}} \left\| \mathbf{\Psi} \right\|_*,$$

where $\gamma_1, \gamma_2 > 0$ are two tuning parameters.

This is a convex programming problem and can be easily solved despite the high dimensionality. This step provides consistent estimation of $\mathbf{B}$ when $\gamma_1, \gamma_2 \to 0$ asymptotically as $(T, p) \to \infty$. However, it introduces a non-trivial shrinkage bias, leading to a non-standard distribution in the slope coefficient estimation. To reduce the bias, we must refine our estimator, which in turn requires determining the number of factors. That motivates the next step.

(b) Estimate the number of factors r by the singular value thresholding:

$$\widehat{r} = \sum_{i=1}^{\min(N,T)} \mathbb{I}\left\{ \psi_i(\widetilde{\mathbf{\Psi}}) \geq \left(\gamma_2 \sqrt{NT} \|\widetilde{\mathbf{\Psi}}\|_2\right)^{1/2} \right\}, \tag{A1}$$

where $\psi_i(\widetilde{\mathbf{\Psi}})$ is the i-th singular value of $\widetilde{\mathbf{\Psi}}$.

(c) To estimate the factor, we first carry out a singular value decomposition of the $N \times T$ matrix $\widetilde{\mathbf{\Psi}} = \underset{(N\times N)}{\widetilde{\mathbf{U}}} \underset{(N\times T)}{\widetilde{\mathbf{D}}} \underset{(T\times T)}{\widetilde{\mathbf{V}}'}$, where $\widetilde{\mathbf{D}}$ stores all singular values, and $\widetilde{\mathbf{U}}$ and $\widetilde{\mathbf{V}}$ are unitary matrices. We obtain a preliminary estimate of $\mathbf{F}$ as the $T \times \widehat{r}$ matrix $\widetilde{\mathbf{F}} = \sqrt{T}\widetilde{\mathbf{V}}_{[\widehat{r}]}$, where $\widetilde{\mathbf{V}}_{[\widehat{r}]}$ is the first $\widehat{r}$ columns of $\widetilde{\mathbf{V}}$.

The second-step estimator (Lasso): We again encourage sparsity when estimating the slope coefficients. We do not penalize the factor loadings, which is the common practice in estimating the interactive fixed effects with a large N. We solve the Lasso problem:

$$\left(\check{\mathbf{B}}, \check{\mathbf{\Lambda}}\right) = \underset{(\mathbf{B},\mathbf{\Lambda})}{\operatorname{argmin}} \frac{1}{2T} \left\| \widetilde{\mathbf{Y}} - \mathbf{B}\widetilde{\mathbf{X}} - \mathbf{\Lambda}\widetilde{\mathbf{F}} \right\|_{\mathcal{F}}^2 + \gamma_3 |\mathrm{vec}(\mathbf{B})|_1,$$

where γ_3 is a tuning parameter. We obtain $\check{\mathbf{B}} = (\check{\mathbf{A}}_1, \ldots, \check{\mathbf{A}}_p)$ and $\check{\mathbf{\Lambda}}$. The purpose of the second step is to refresh the first-step consistent slope coefficient estimator.

The third-step estimator (Conservative Lasso):

(a) Set $\widehat{\mathbf{F}}^{(0)} = \widetilde{\mathbf{F}}$. Let $\ell = 1$, and update the estimates of $\mathbf{B} = (\mathbf{A}_1, \ldots, \mathbf{A}_p)$ and $\mathbf{\Lambda}$ using:

$$\left(\widehat{\mathbf{B}}^{(\ell)}, \widehat{\mathbf{\Lambda}}^{(\ell)}\right) = \underset{(\mathbf{B},\mathbf{\Lambda})}{\operatorname{argmin}} \frac{1}{2T} \left\| \widetilde{\mathbf{Y}} - \mathbf{B}\widetilde{\mathbf{X}} - \mathbf{\Lambda}\widehat{\mathbf{F}}^{(\ell-1)} \right\|_{\mathcal{F}}^2 + \gamma_4 \sum_{k=1}^{p} \sum_{i,j\in[N],j\neq i} w_{i,j} \left| A_{i,j,k} \right|,$$

where $w_{i,j} = \mathbb{I}\left\{\left|\check{A}_{i,j,k}\right| < \gamma_4\right\}$ for all $k \in [p]$ and γ_4 is a tuning parameter. This step imposes a large penalty on true zero parameters and spares the diagonal elements from the penalty.

(b) Update $\widehat{\mathbf{F}}^{(\ell)}$ using the singular value decomposition $\widetilde{\mathbf{\Psi}}^{(\ell)} = \widetilde{\mathbf{Y}} - \widehat{\mathbf{B}}^{(\ell)}\widetilde{\mathbf{X}} = \widehat{\mathbf{U}}^{(\ell)}\widehat{\mathbf{D}}^{(\ell)}\widehat{\mathbf{V}}^{(\ell)\prime}$, and then $\widehat{\mathbf{F}}^{(\ell)} = \sqrt{T}\widehat{\mathbf{V}}^{(\ell)}_{[\widehat{r}]}$.

(c) Set $\ell = \ell + 1$. Iterate steps (a)-(b) for a finite time $\ell^{\max}$. Denote the final estimates by $\widehat{\mathbf{B}} = \widehat{\mathbf{B}}^{(\ell^*)}$, $\widehat{\mathbf{F}} = \widehat{\mathbf{F}}^{(\ell^*-1)}$, and $\widehat{\mathbf{\Lambda}} = \widehat{\mathbf{\Lambda}}^{(\ell^*)}$.

A.2 VAR Lag Selection

Set a maximum number $p_{\max} > p^0$ to estimate the model, where we use the superscript "0" to denote the true lag. The model with $p_{\max}$ lags is still a correctly specified model, but $\mathbf{A}_k^0 = \mathbf{0}$ is redundant for $k > p^0$. Due to Lasso regularization, the estimates $\widehat{\mathbf{A}}_p$ for $p > p^0$ should converge to zero. Therefore, we use the following procedure to determine the lag length:

(a) Estimate the model with lag $p_{\max}$ and obtain the estimates $\widehat{\mathbf{A}}_k$ for $k \in [p_{\max}]$.

(b) Calculate $a_k = \max\{\|\widehat{\mathbf{A}}_k\|_{\mathcal{F}}^2, c\}$ for some small positive constant c.

(c) For each $p \in [p_{\max} - 1]$, compute the ratio $GR(p) = \sum_{k=p}^{p_{\max}} a_k \big/ \sum_{k=p+1}^{p_{\max}} a_k$

(d) Obtain the estimator number of lags as the maximizer of $GR(p)$.

A.3 Normalization of the Factor Loadings and Common Factor

In the empirical analysis, our model selects one common factor, i.e., $\widehat{r} = 1$, by the data-driven procedures above. To simplify the notation, we use $\underset{(N\times 1)}{\mathbf{\Lambda}}$ to denote the factor loadings. We normalize

the factor loadings as $\mathbf{\Lambda}^{\text{normalized}} = \mathbf{\Lambda}/\bar{\lambda}$, where $\bar{\lambda} = \mathbf{w}'\mathbf{\Lambda}$ is the weighted mean of the factor loadings and $\mathbf{w} = (w_i)_{i=1}^N$ are the consumption basket weights of PCE of N sectors. Correspondingly, the normalized common factor is $f_t^{\text{normalized}} = \bar{\lambda} f_t$, ensuring that the product of the factor and loadings after normalization equals the original $\mathbf{\Lambda} f_t$.

This normalization not only enhances the interpretability of model parameters (Mayoral and Gadea, 2011), but also facilitates a clearer understanding of the roles and relative importance of common factors and idiosyncratic shocks. Specifically, after normalization, the aggregate impulse responses of the common factors are given by $\mathbf{IR}_\pi^f(h=0) = \mathbf{w}'\mathbf{\Lambda} = 1$ (Eq.(8) in Section 3.2), which aligns with the aggregate impulse responses of the uniform sectoral shock, following Eq.(5) in Section 3.2, $\mathbf{IR}_\pi^{\mathbf{u}}(h=0) \cdot \mathbf{1} = \mathbf{w}'\mathbf{1} = 1$.

B Simulation

We follow the notations in Section 3 and set the lag of our model to $p = 1$. The true autoregressive matrix $\mathbf{A}_1^0$ is defined as a sparse matrix with diagonals equal to 0.6 and each row has two additional random cells with values 0.2 and -0.2, as shown in Figure A1. Data is generated from a VAR(1) system with a single common factor, following Eq.(1):

$$\mathbf{Y}_t = \mathbf{A}_1^0 \mathbf{Y}_{t-1} + \mathbf{\Lambda}^0 f_t^0 + \mathbf{u}_t, \quad t \in [T],$$

where $\mathbf{Y}_t$ is an $N \times 1$ vector, $\mathbf{\Lambda}^0 = (\lambda_i^0)_{i=1}^N$ represents the vector of the factor loadings and $\mathbf{u}_t = (u_{it})_{i=1}^N$ denotes the vector of idiosyncratic shocks. The factor loadings λ_i^0 and the error terms u_{it} ($i \in [N]$) are independently and identically distributed (i.i.d.) standard normal random variables. The common factor f_t^0 follows the autoregressive process given by

$$f_t^0 = \rho^0 f_{t-1}^0 + \epsilon_t,$$

where $\rho^0 = 0.025$, matching the AR(1) coefficient of the estimated common factor, and ϵ_t is i.i.d. and follows a normal distribution.

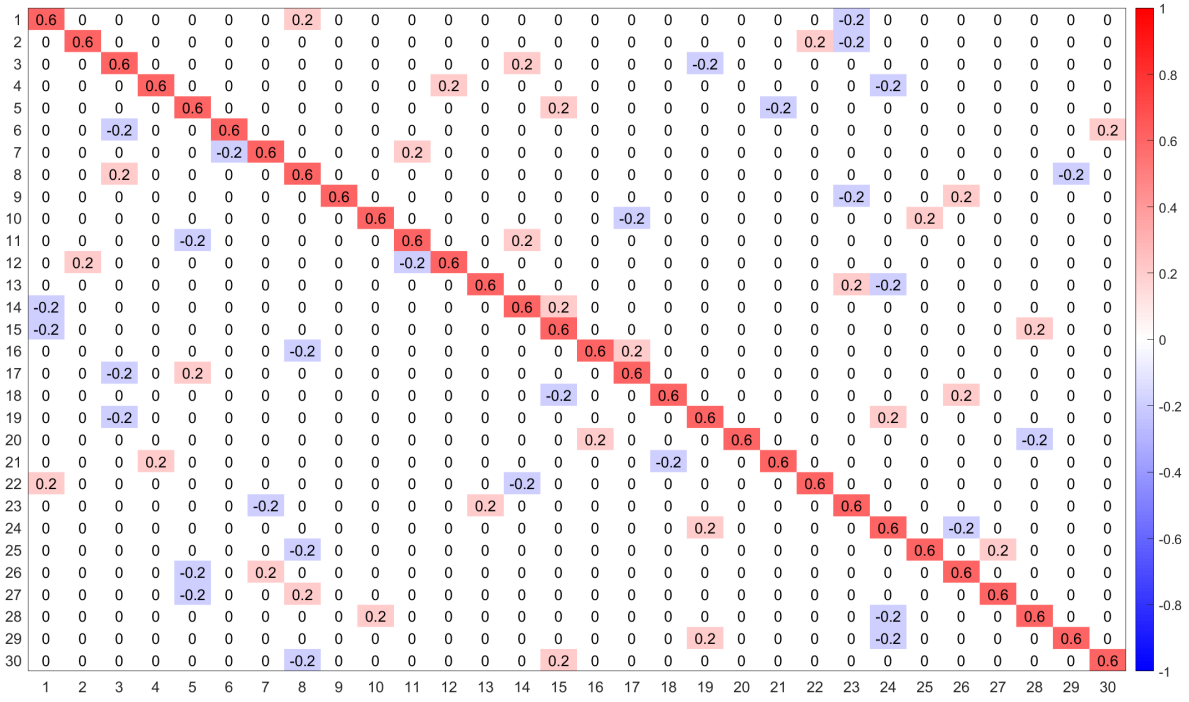


Figure A1: True VAR Matrix

Notes: This heat map presents the true autoregressive coefficient matrix $\mathbf{A}_1^0$. Positive and negative values are represented by the red and blue cells and white cells for no impact.

For such a generating process, we consider $N = 30$, and $T = 500$. We use the VAR(1) model with

a single common factor to estimate. For each generated time series $\mathbf{Y}_t$, we apply two estimations, one is the estimation procedure outlined in Appendix A, and the other is Ordinary Least Squares (OLS) estimation. This simulation is conducted over 500 iterations.

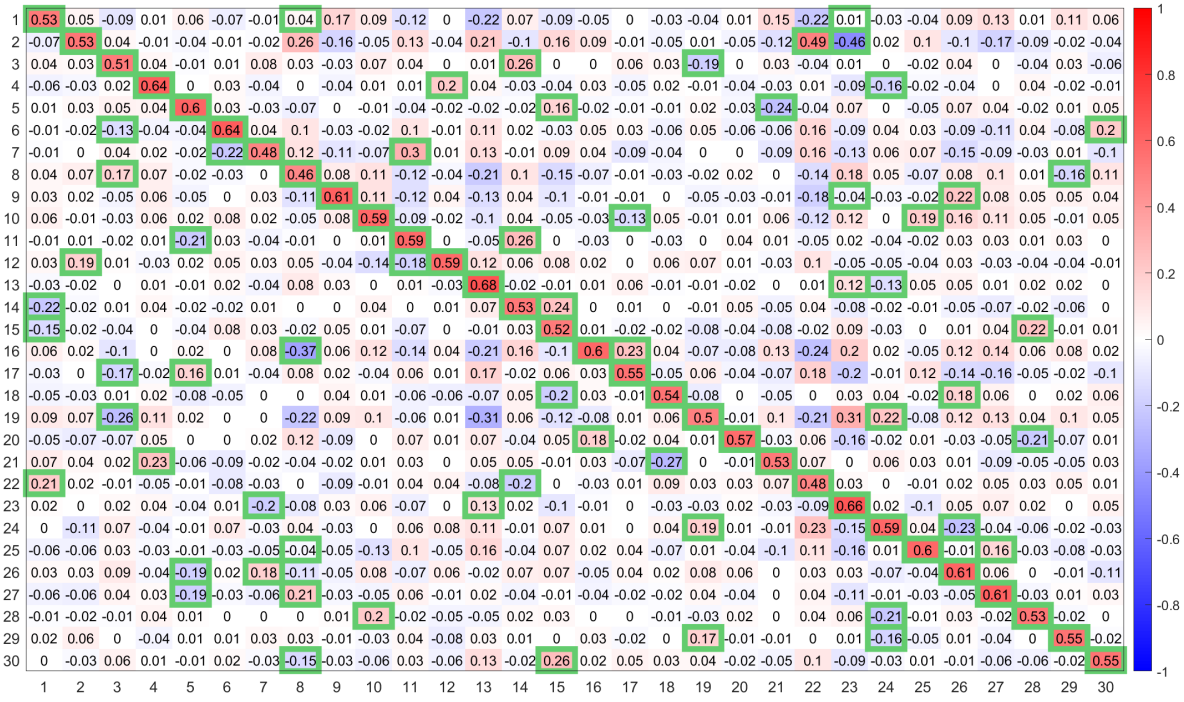


Figure A2: Estimated VAR Matrix without Lasso

Notes: This heat map presents the autoregressive coefficient matrix estimated by OLS from one of 500 simulations. Positive and negative values are represented by the red and blue cells and white cells for no impact. Those non-zero entries of the true autoregressive coefficient matrix $\mathbf{A}_1^0$ are highlighted in green.

The two figures reveal distinct differences in estimation performance. In Figure A2 (without Lasso), many non-zero coefficients appear in positions where the true autoregressive matrix $\mathbf{A}_1^0$ has zero entries, indicating the introduction of spurious coefficients. In contrast, Figure A3 (with Lasso) shows a much sparser matrix, with most non-zero coefficients aligning with the true non-zero entries of $\mathbf{A}_1^0$. Lasso effectively reduces spurious non-zero estimates and improves the accuracy of the estimated coefficients, especially in the true non-zero positions. Overall, Lasso captures the sparse structure of the true matrix more accurately than OLS, making it a superior method for sparse modeling.

Table A1 highlights the advantages of using Lasso for estimating the VAR matrix. While both methods achieve a 100% true positive rate (TPR), Lasso significantly reduces the false positive rate (FPR) from 100% to 8.96%, indicating better sparsity recovery and fewer spurious non-zero estimates. Additionally, Lasso achieves much lower root mean squared errors (RMSEs) for both all entries (0.0001 vs. 0.0027) and non-zero entries (0.0009 vs. 0.0038), demonstrating its superior accuracy in estimating the coefficients. These results underscore the effectiveness of Lasso in

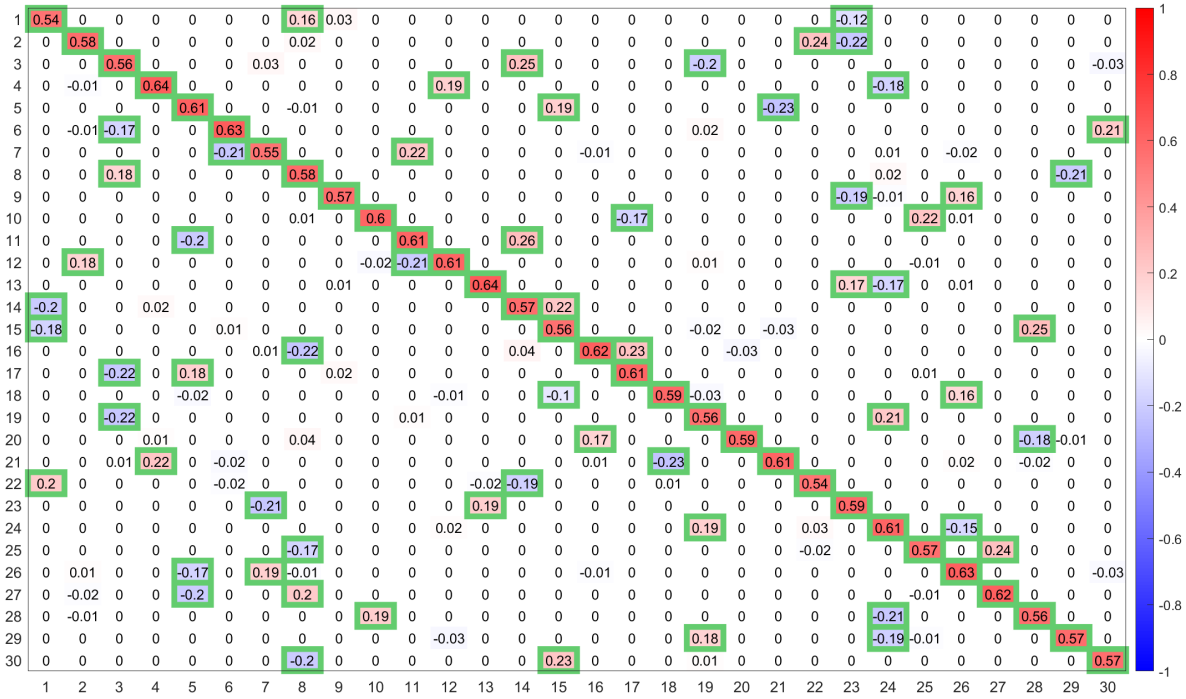


Figure A3: Estimated Autoregressive Matrix with Lasso

Notes: This heat map presents the autoregressive coefficient matrix using the estimation procedure in Appendix A from one of 500 simulations — the same simulation as Figure A3. Positive and negative effects are represented by the red and blue cells and white cells for no impact. Those non-zero entries of the true autoregressive coefficient matrix $\mathbf{A}_1^0$ are highlighted in green.

capturing the true sparse structure of the autoregressive matrix while minimizing estimation errors.

Table A1: Model Selection Accuracy and Root Mean Squared Errors (RMSEs) of the VAR Matrix

N	T		Without Lasso	Lasso
30	500	RMSEs	0.0027	0.0001
		RMSEs (Nonzero entries)	0.0038	0.0009
		TPR	100%	100%
		FPR	100%	8.96%

Notes: This table presents the RMSEs of the autoregressive matrix and the model selection accuracy by true positive rate (TPR) and false positive rate (FPR). The RMSEs for all entries and nonzero entries in the true autoregressive matrix $\mathbf{A}_1^0$ are reported respectively. The TPR reports the average percentage that non-zero entries of the true autoregressive matrix $\mathbf{A}_1^0$ are estimated to be non-zero. The FPR reports the average percentage that zero entries of the true autoregressive matrix $\mathbf{A}_1^0$ are estimated to be non-zero.

C Estimated Autoregressive Matrix without Lasso

To show the importance of using the Lasso method to improve the estimation of the FAVAR model, we present the estimated autoregressive matrix without using Lasso in Figure A4. The heatmap shows that the majority of the off-diagonal elements are non-zero, which mirrors the results of Figure A2 we observed in our simulations. The presence of these non-zero correlations may lead to an overestimation of the spillover among sectors and may exaggerate the impact of one sector on another.

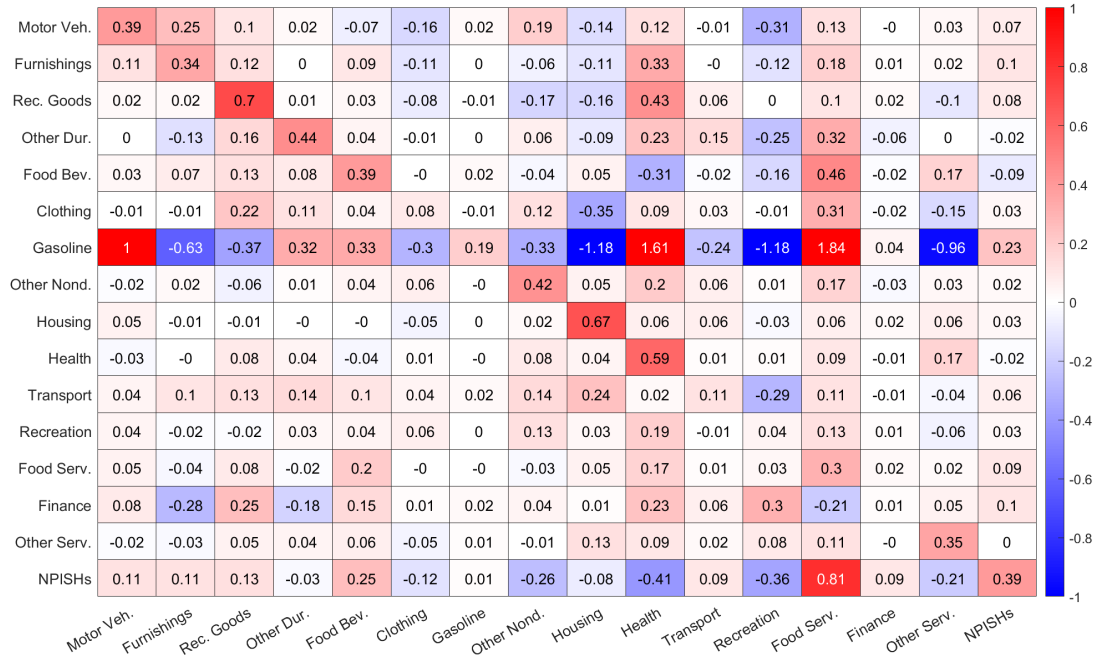


Figure A4: Autoregressive Matrix without Lasso

Notes: This heat map presents the estimated autoregressive coefficient matrix without Lasso. Positive and negative effects are represented by the red and blue cells and white cells for no impact.

D Ranking of Sectoral Inflation Persistence

Table A2: Ranking of Sectoral Inflation Persistence

Sector	$\widehat{a}_{ii}$	Sector	$\widehat{a}_{ii}$
Housing and utilities	0.88	Final consumption expenditures of nonprofit institutions serving households (NPISHs)	0.38
Recreational goods and vehicles	0.76	Food services and accommodations	0.34
Health care	0.68	Furnishings and durable household equipment	0.31
Other nondurable goods	0.49	Gasoline and other energy goods	0.18
Other services	0.43	Recreation services	0.16
Other durable goods	0.43	Transportation services	0.14
Motor vehicles and parts	0.40	Clothing and footwear	0.09
Food and beverages purchased for off-premises consumption	0.39	Financial services and insurance	0.04

Notes: This table ranks the diagonal entries $\widehat{a}_{ii}$ $(i \in [N])$ of the estimated autoregressive coefficient matrix $\widehat{\mathbf{A}}_1$ from the largest to the smallest, which capture the impact of each sector's inflation in the previous period on its own inflation in the current period.

E Eigenvalues of the Estimated VAR Matrix

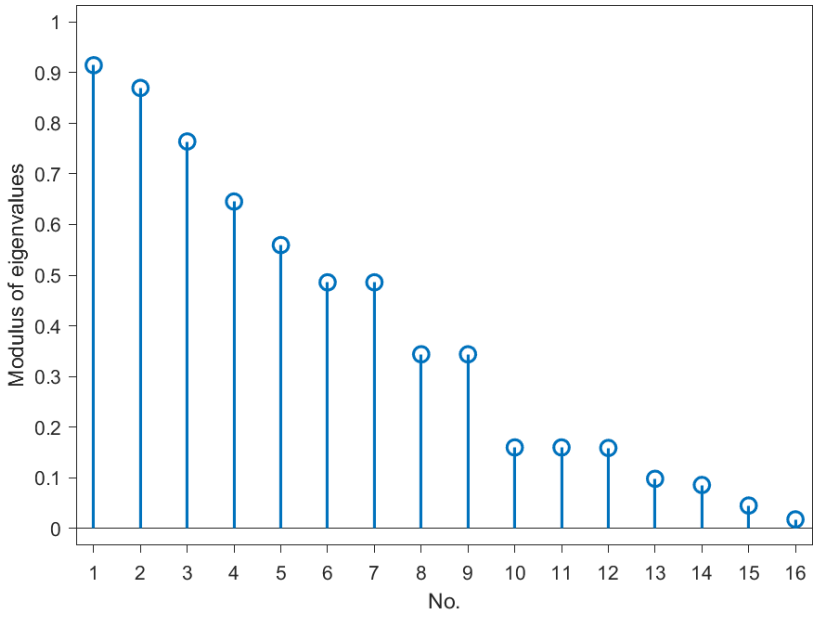


Figure A5: Modulus of the Eigenvalues of the Vector Estimated Autoregressive Matrix $\widehat{\mathbf{A}}_1$ (Descending)

F Procedure of Constructing Production I-O Matrix

Commodity-by-commodity I-O table. We obtained the detailed commodity-by-commodity I-O table from the Bureau of Economic Analysis (BEA) titled "Commodity-by-Commodity Total Requirements, After Redefinitions", which encompasses 402 commodities. This table presents the total inputs required by commodity (both directly and indirectly) to deliver one dollar of commodity output to final users. For the detailed level, BEA provides I-O tables for the years 2007, 2012, and 2017. Given the similarities of the results across these three tables, we select the 2012 table for our analysis.

PCE bridge table. BEA also provides the PCE bridge table, which outlines the commodity composition of PCE. We utilize the purchasers' value from the PCE bridge table for the same year to establish the relationship between the detailed commodity items and the 16 PCE sectors.

Construction Procedure:

(a) Acquire the detailed commodity-by-commodity I-O table IO, which is a 402 by 402 matrix.

(b) Construct a 16 by 402 bridge matrix B using the purchasers' value from the PCE bridge table, where the rows and columns correspond to the PCE sectors and the detailed commodities. Each row of the bridge matrix is normalized so that the sum of each row equals one; thus, the entry b_{ij} represents the proportion of commodity j within the respective PCE sector i.

(c) Condense the detailed commodity-by-commodity I-O table IO to the 16×16 I-O matrix A_{IO} using the bridge matrix B via $A_{IO} = B \times IO \times B^T$.

G Aggregate Inflation Impulse Responses to Each Sectoral Shock

We examine the impulse response of aggregate inflation to sectoral shocks. Figure A6 presents a striking illustration of the significant heterogeneity in how aggregate inflation responds to a 1% inflation shock originating from each sector. Note that the initial responses to each sectoral shock naturally equal the respective sectoral weights in the price index.

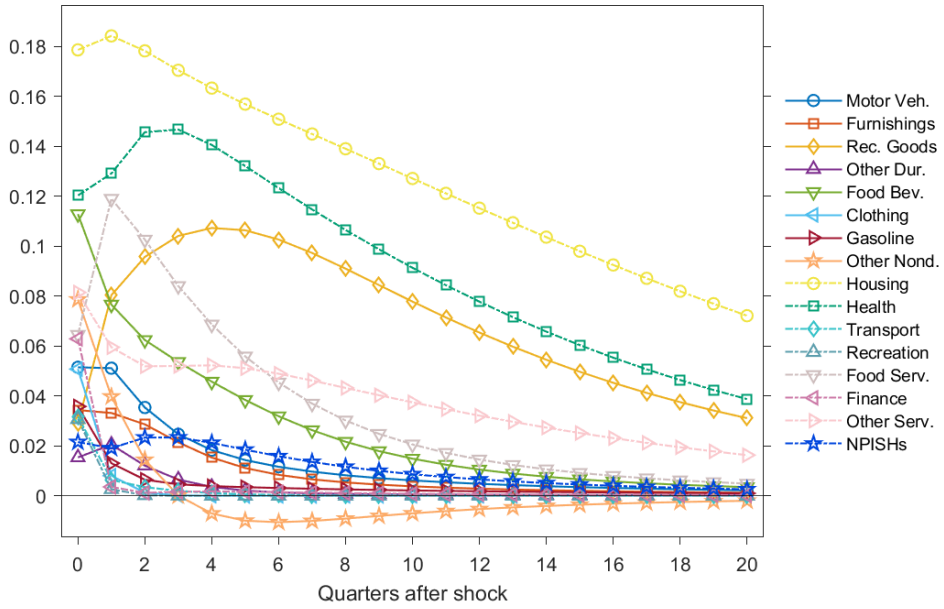


Figure A6: Aggregate Impulse Responses to Sectoral Shocks

Notes: This figure presents impulse responses of aggregate inflation to 1% sectoral shock from 16 sectors for $h = 1, ..., 20$.

The dynamics of the aggregate inflation IRFs reveal some notable departures from the monotonic decay that would be anticipated in the absence of sectoral spillover effects for certain sectors. For example, for shocks originating from "Recreational goods and vehicles" and "Health care", the aggregate inflation IRFs continue to rise for an extended period, extending over 9 months and even up to a full year. Similarly, the sectoral shocks in the sectors of "Housing and utilities" and "Food services and accommodations" also exhibit an initial increase in their impact on aggregate inflation before gradually declining.

By contrast, the impacts of some sectoral inflation shocks are short-lived and have limited effects on aggregate inflation. This is the case for sectors like "Clothing and footwear", "Recreation services", "Other nondurable goods", "Other durable goods", and "Financial services". Surprisingly, the shock to "Gasoline and other energy goods" has a very small effect on aggregate inflation, possibly attributed to the fact that the estimated common shocks are associated with the fluctuations in crude oil prices, which will be discussed in more detail later.

H Lag Selection for Estimated Common Factor Fitting AR Model

To capture the persistence in the common factor, this table presents the Bayesian Information Criterion (BIC) values for selecting the lag order in an AR(d) model for fitting the estimated common factor.

$$\text{BIC} = \ln \widehat{\sigma}^2 + \frac{\ln(T)}{T} d$$

where T is the number of observations and $\widehat{\sigma}^2$ is the residual variance estimate. The optimal lag order, denoted with an asterisk (*), is at lag 0, with the lowest BIC value.

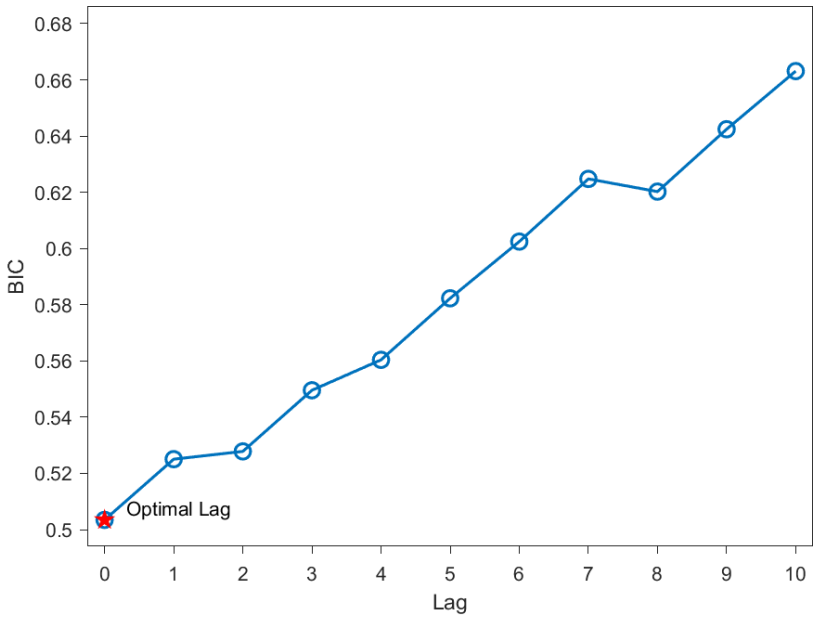


Figure A7: Lag Order Selection Criteria for Estimated Common Factor

Notes: This figure presents the lag order selection criteria BIC for the estimated common factor fitting AR(p) model. The maximum lag is 10, with the red star representing the optimal lag.

I Alternative Approach to Evaluating Spillover

In previous sections, we conduct counterfactual experiments to evaluate the role of inter-sectoral spillover and sectoral heterogeneity in aggregate inflation persistence. An alternative approach is to estimate restrictive models without those features and compare the corresponding IRFs to sectoral and common shocks. More specifically, we estimate the following two restrictive models:

(a) Heterogeneous autoregressive coefficients without spillover:

$$\mathbf{Y}_t = \mathbf{A}_1 \mathbf{Y}_{t-1} + \mathbf{\Lambda} f_t + \mathbf{u}_t,\ t = 1, ..., T \tag{A2}$$

where $\mathbf{A}_1$ is a diagonal matrix.

(b) Homogeneous autoregressive coefficients without spillover:

$$\mathbf{Y}_t = a_1 \mathbf{Y}_{t-1} + \mathbf{\Lambda} f_t + \mathbf{u}_t,\ t = 1, ..., T \tag{A3}$$

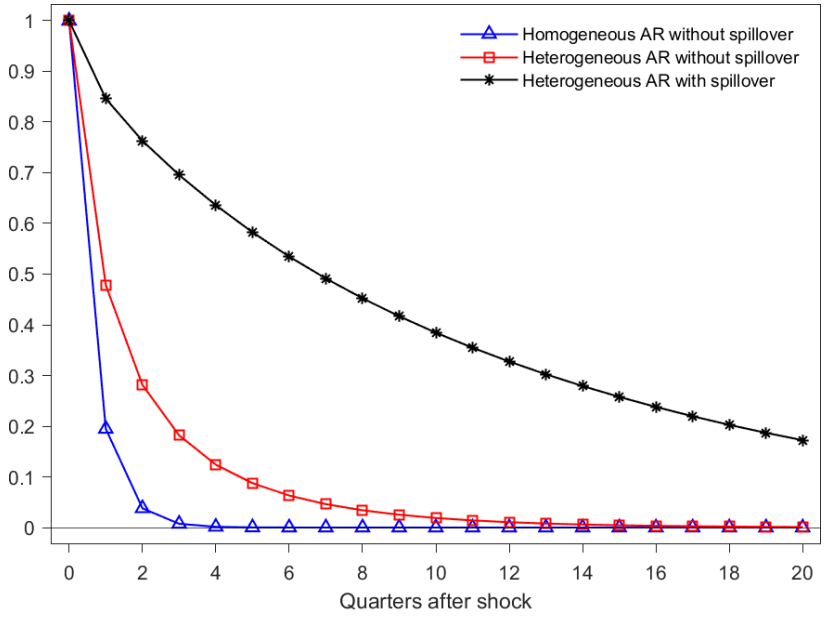
where a_1 is a scalar.

Model (a) is designed to assess the impact of shutting down sectoral spillover while retaining sectoral persistence heterogeneity, whereas Model (b) assumes homogeneous sectoral persistence with no spillover effects. For ease of comparison with our baseline model, we maintain consistency by setting the number of common factors to 1 when estimating these two restrictive models, aligning with the estimates of our general model.

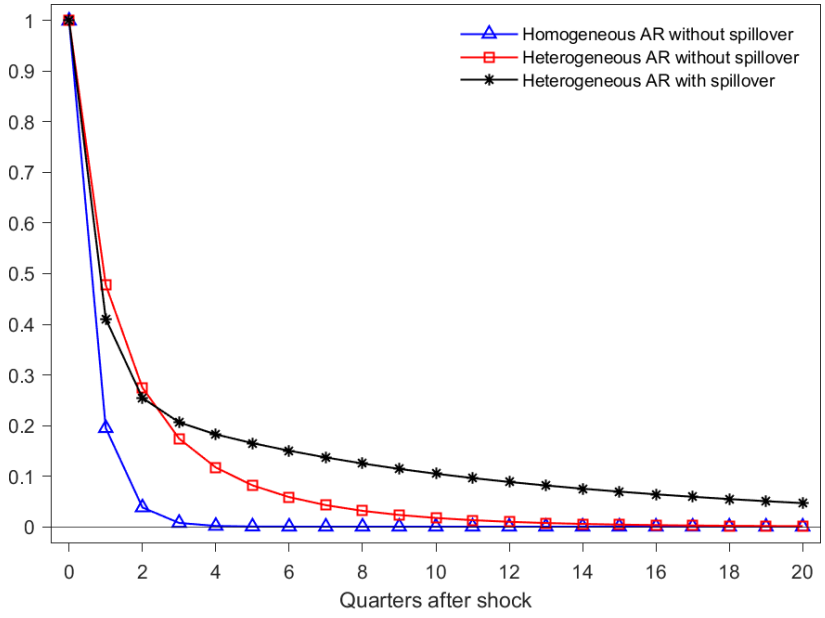
After estimating these three models, we compute the impulse responses of aggregate inflation to 1% uniform sectoral shock and 1% common shock. The resulting IRFs are displayed in Figure A8, allowing for a direct comparison of how different modeling assumptions affect aggregate inflation dynamics.

Figure A8 presents a similar pattern in our previous counterfactual experiments for uniform sectoral shocks and common shocks in Figure 9 and Figure 11. First, our general model, which incorporates inter-sectoral spillover effects, has higher persistence as a response to both uniform sectoral shocks and common shocks compared with the two restrictive models, particularly for sectoral shocks. Second, although both shocks are temporary, the longer-term effects of both shocks remain evident, as indicated by the impulse response of aggregate inflation still standing at 18 and 5 basis points five years after the initial shock at sectoral or aggregate level, respectively.

By contrast, the performance of the two restrictive models falls short of adequately capturing the persistence of aggregate inflation. In the homogeneous autoregressive coefficients model without spillover, the impulse responses of aggregate inflation to two types of shocks nearly vanish within a year, with the IRFs quickly declining to zero. This outcome underscores the limitation of ignoring inter-sectoral spillover and sectoral heterogeneity.



(a) Aggregate Impulse Responses to Uniform Sectoral Shocks



(b) Aggregate Impulse Responses to Common Shock

Figure A8: Comparing with Two Restrictive Models

Notes: This figure presents impulse responses of aggregate inflation to 1% uniform sectoral shock (Panel (a)) and common shock (Panel (b)) using different models for $h = 1, ..., 20$. The black line represents the baseline IRFs. The blue line marked with triangles represents the restrictive model Eq.(A2) eliminating heterogeneous sector self-persistence and spillover effects. The red line marked with squares represents the restrictive model Eq.(A3) allowing for heterogeneous sector self-persistence but eliminating spillover effects.

Similarly, in the model that only accounts for sectoral heterogeneity while ignoring inter-sectoral spillover, the IRF of aggregate inflation reduces to one-tenth the size of the initial shock approximately four quarters following a uniform sectoral or a common shock. Subsequently, the reduction in IRFs accelerates significantly, and the impact almost vanishes after three years. However, the model with heterogeneous autoregressive coefficients without spillover still demonstrates relatively more persistent IRFs than the homogeneous autoregressive coefficients model without spillover, indicating that sectoral heterogeneity in persistence still plays a role in increasing aggregate inflation persistence; however, its role is quite limited compared with the spillover.

J Sources of Aggregate Inflation in Great Inflation Period

Utilizing the previously mentioned decomposition, we attempt to comprehend the drivers contributing to inflation during the Great Inflation. The contribution of sectoral and common shock components to aggregate inflation from 1970Q1 to 1985Q4 is depicted in Figures A9 and A10.

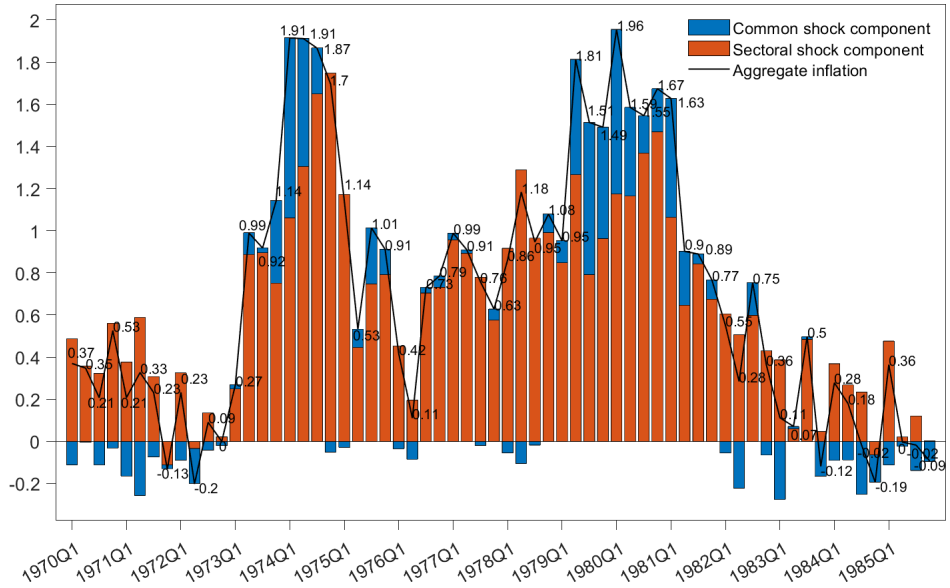


Figure A9: Decomposition of Aggregate Inflation: Great Inflation Period

Notes: This figure presents the breakdown of the demeaned quarter-on-quarter aggregate inflation (black line) into the sectoral component (red bars) and common shock component (blue bars) in the Great Inflation period from 1970Q1 to 1985Q4. The numbers on the black line represent the demeaned quarter-on-quarter aggregate inflation.

During the early years of this period, which lasted from 1970Q1 to 1972Q4, aggregate inflation was relatively constant. However, there were indications of rising volatility during this time, mostly caused by sectoral shocks. Throughout this time, the sector shock component remained remarkably consistent and mostly positive, indicating that inflation was progressively driven by sector-specific forces. Increased demand, subpar harvests, and global agricultural disruptions raised food costs, a significant factor in early 1970s inflation.

Inflation sharply rose between 1973Q1 and 1976Q2 and reached the first peak, propelled by both common and sectoral shocks. The 1973 oil embargo imposed by the Organization of Arab Petroleum Exporting Countries (OAPEC) caused oil prices to spike sharply, which significantly affected the common shock component. Furthermore, the sectoral shock component grew, particularly impacting energy-dependent industries like manufacturing and transportation, whose production costs surged as a result of the spike in oil prices. Food prices continued to rise due to the ongoing global food scarcity and growing expenses for agricultural inputs. Inflationary pressures also affected

the price of homes, particularly the cost of building and upkeep. On average, the sectoral shock component contributed 82.5% of aggregate inflation during the peak period (1973Q1-1974Q3), while the common shocks component accounts for just 17.5%. Aggregate inflation gradually declined after 1974Q4. Such a large contribution indicates that sector shocks were a much bigger factor in this period's inflation than the general belief that oil prices were the only factor.

By the late 1970s (1976Q3 to 1979Q1), the common shock component was more volatile, reflecting ongoing economic adjustments. The sector shock component continued to be the key driver of inflation, contributing positively with time and showing less volatility than it did in the middle of the 1970s.

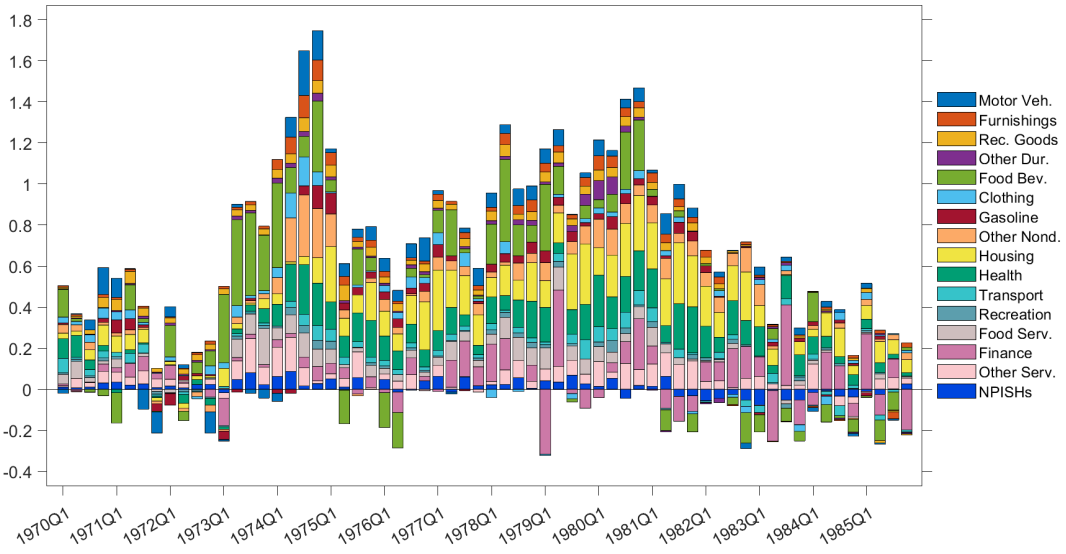


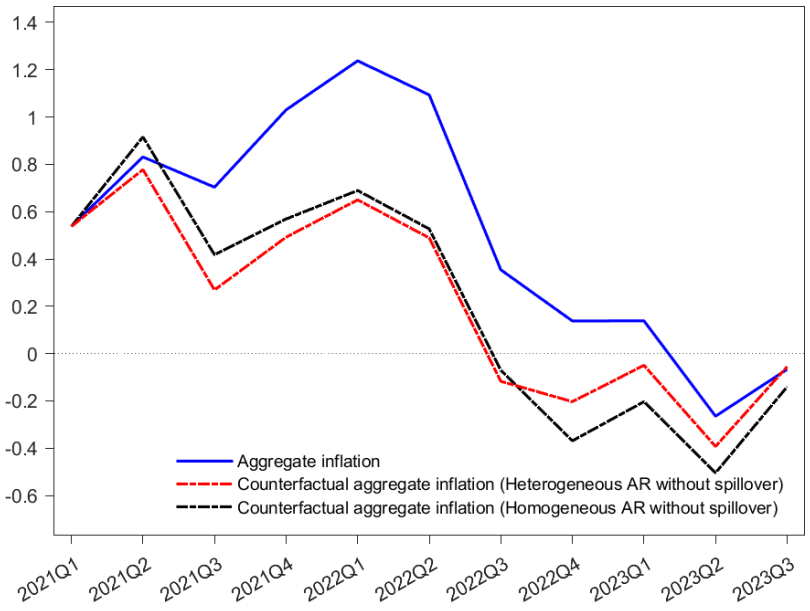
Figure A10: Decomposition of Sectoral Shock Component: Great Inflation Period

Notes: This figure presents the decomposition of the sectoral shock component into 16 distinct sectors in the Great Inflation period from 1970Q1 to 1985Q4.

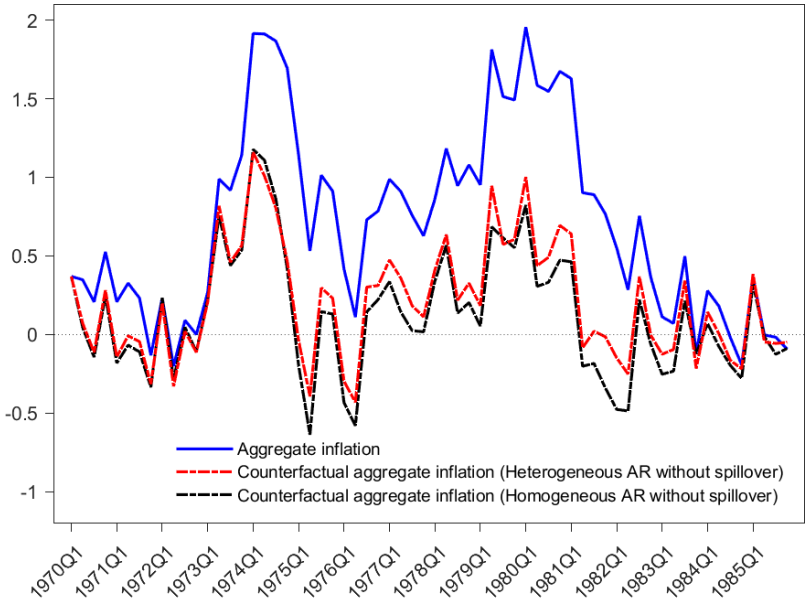
Between 1979Q2 and 1981Q1, inflation peaked for the second time. The Iranian Revolution and other geopolitical events precipitated the second oil shock of 1979, which increased oil prices and made the common shock component worse. Sector shock components, such as severe price increases in the food, housing, and energy sectors, also had a significant impact. Restricted supply had a particularly negative impact on the energy sector, while tight monetary policy and rising interest rates drove up housing costs. During this peak period, the sectoral shock component had an average contribution of 70.2% to aggregate inflation, whereas the common shocks component only accounted for 29.8%.

Aggregate inflation started to decrease from 1981Q2, mostly as a result of fewer common shocks. This time frame matched the Federal Reserve's vigorous monetary tightening, which involved the application of high interest rates to combat ongoing inflation. Because of these measures, economic activity slowed down and inflationary pressures decreased. Nonetheless, sectoral shocks persisted, especially in the housing sector, which hampered the overall decrease in inflation.

K Robustness of Counterfactual Results: Two Common Factors



(a) Post-COVID-19 Period



(b) Great Inflation Period

Figure A11: Aggregate Inflation with and without Spillover in Great Inflation Period and Post-COVID-19 Period (Set the Number of Common Factors Equal to Two)

Notes: This figure presents the actual demeaned quarter-on-quarter aggregate inflation (blue solid line) and two counterfactual counterparts in the post-COIVD period (2021Q1-2023Q3) and the Great Inflation period (1970Q1-1985Q4). The black dashed line eliminates heterogeneous sector self-persistence and spillover effects. The red dashed line allows for heterogeneous sector self-persistence but eliminates spillover effects.